

SEA ICE: HISTORY

MAJOR CONTRIBUTIONS:-

F. NANSEN - "FRAM" 1893 - 95

H.SVERDRUP "MAUD" - 1923-24

SOVIET RESEARCH - NORTHERN SEA ROUTE

- "NORTH POLE" STATIONS 1937-9, 1951-91

CLASSIC BOOK by ZUBOV "Sea Ice" (1945, trans. 1963)

U.S. ICE ISLAND STATIONS (late 1950s-60s)

SUBMARINE DATA - "Nautilus" 1958, "Queenfish" 1970

AERIAL RECONNAISSANCE (1950s-->) ; SATELLITES (1960s-->)

ARCTIC DRIFTING BUOY PROGRAM 1979-->

FIELD PROGRAMS:

AIDJEX 1974-76

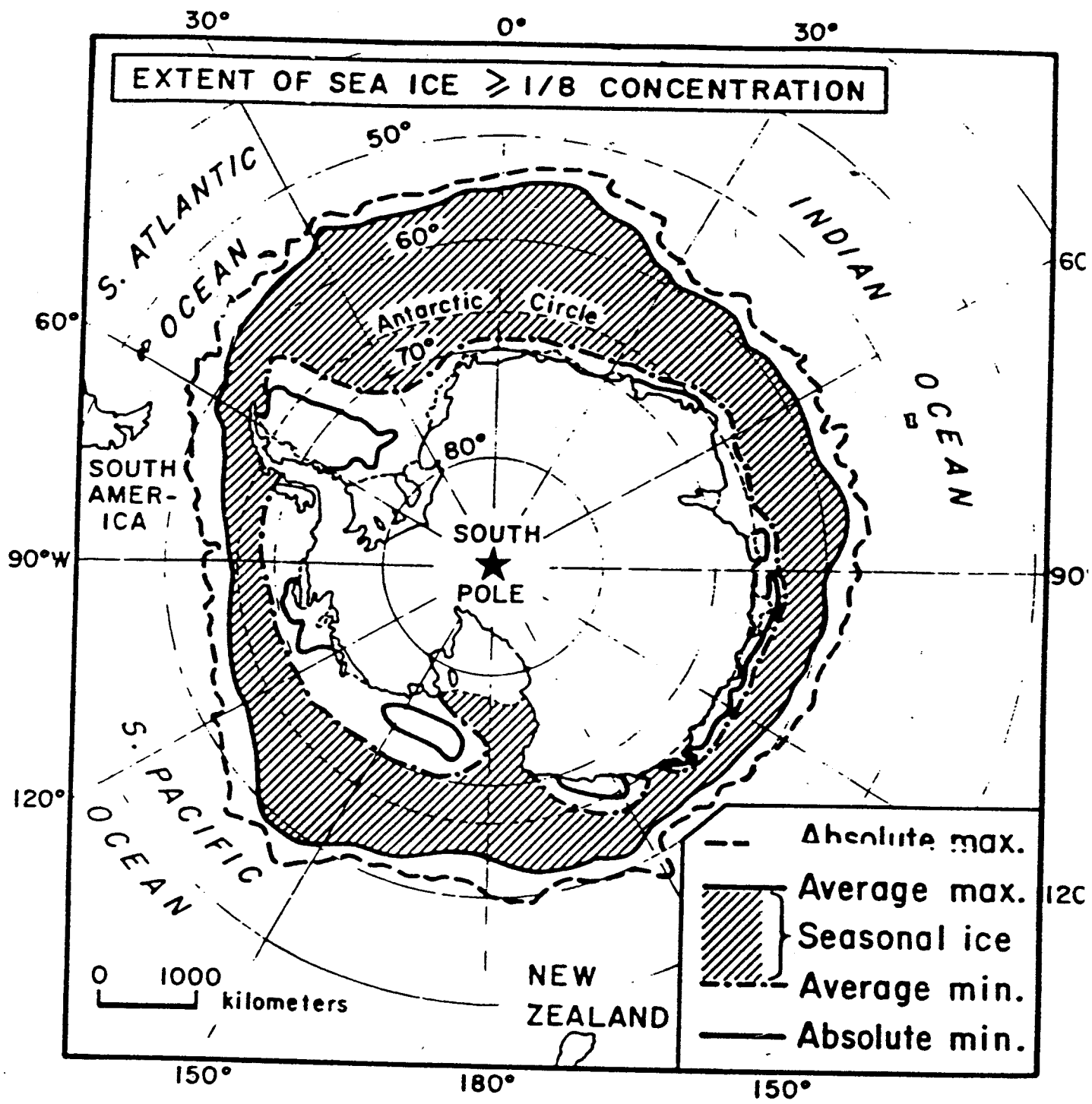
MIZEX, CEAREX 1980s

LEADEX 1992-3

WEDDELL SEA DRIFTING STATION 1993

ICEBREAKER CRUISES - Polarstern, Odin, USCG ships, Russian

SHEBA Station 1997/8



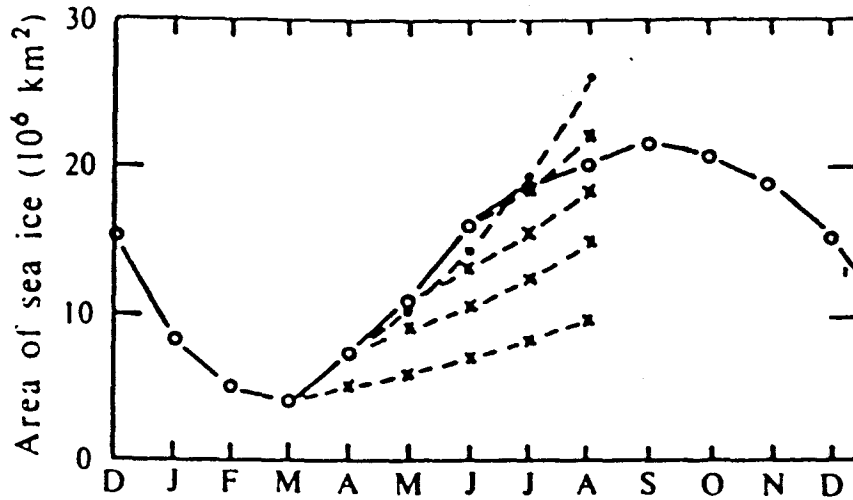
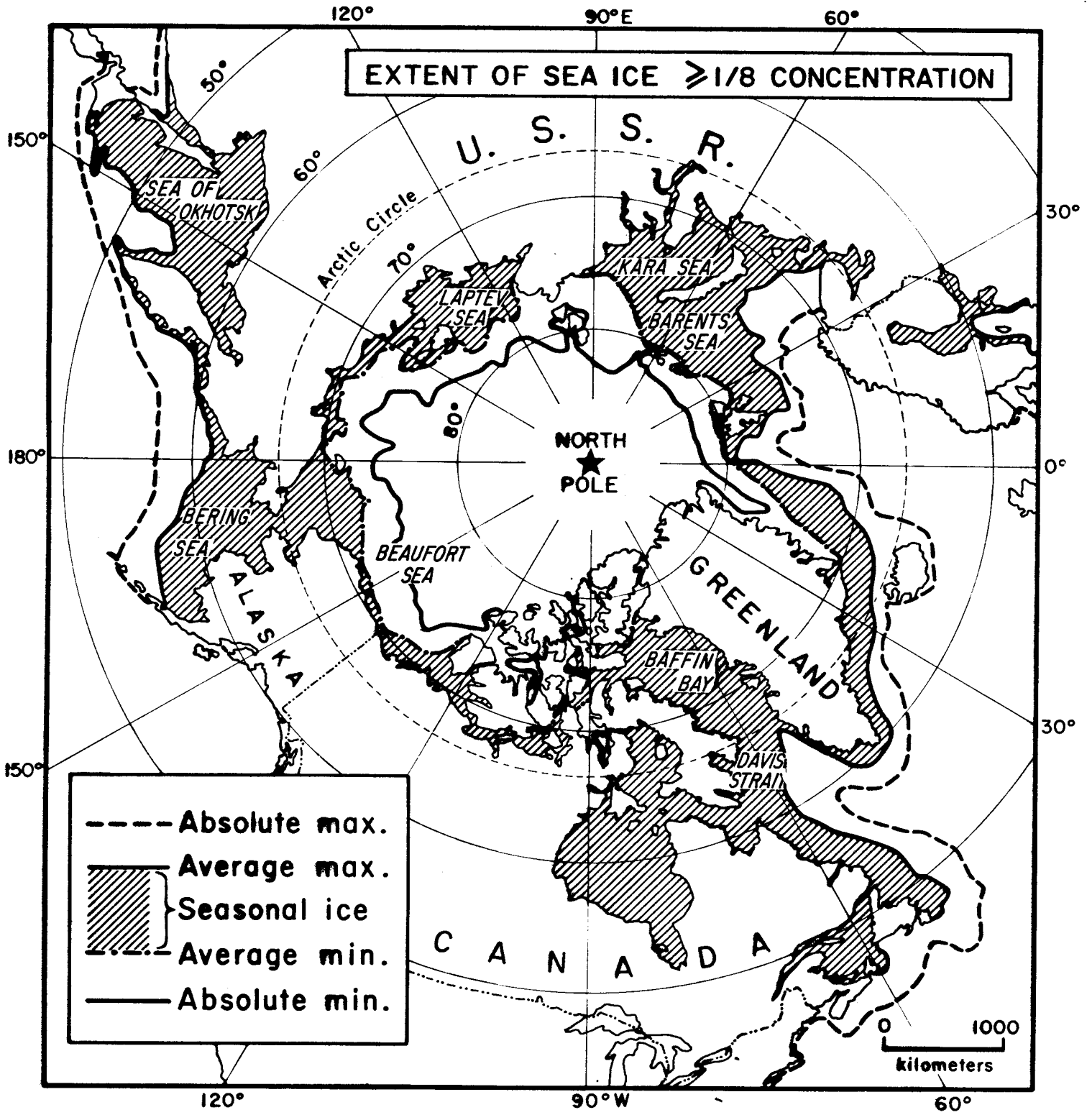
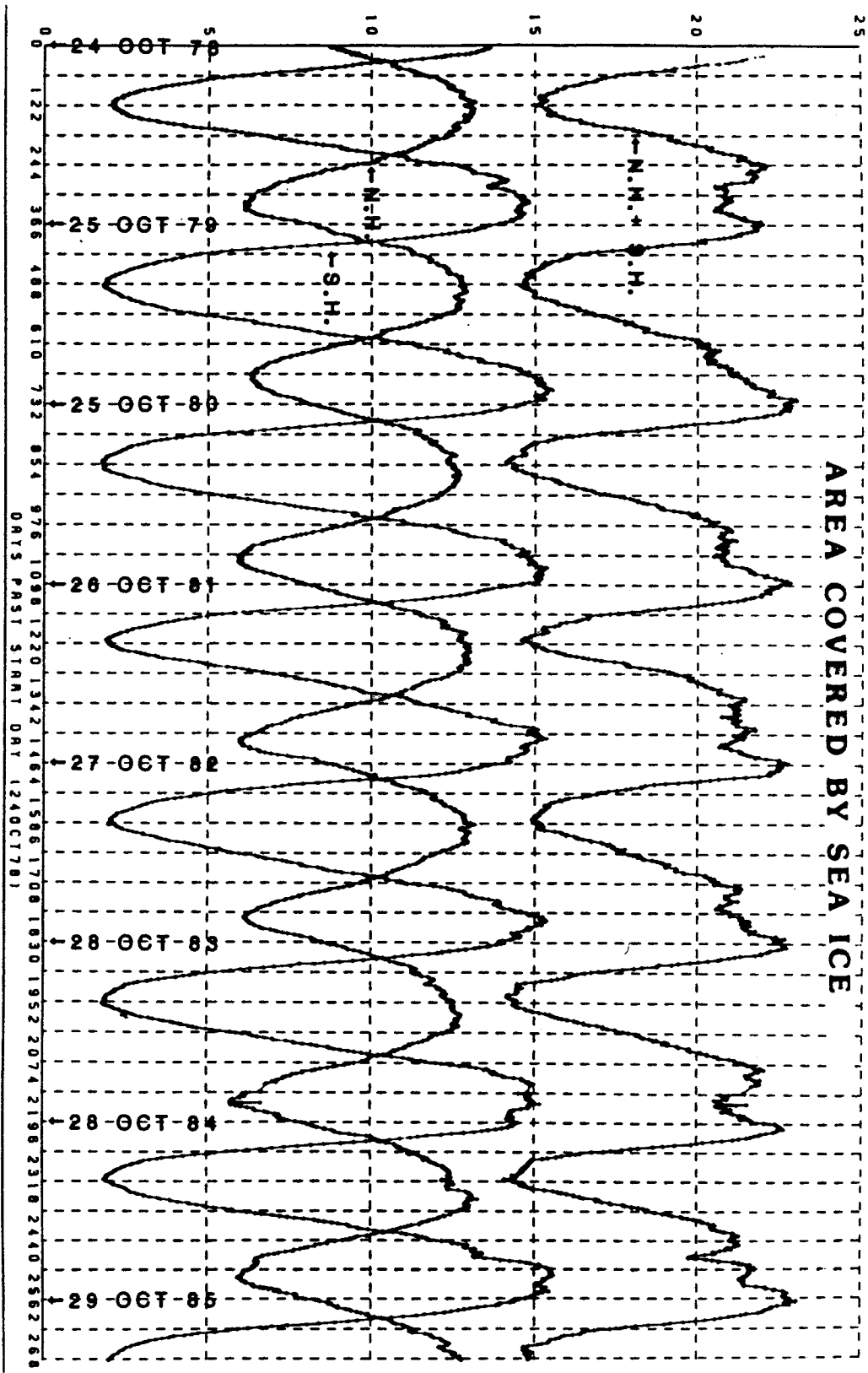


Figure 9: (O) annual fluctuation of Antarctic sea ice. (Solid Curve). The other curves show the sea ice area during advance based on Ekman divergence with a drag coefficient of 1.3×10^{-3} (x) or 2.6×10^{-3} (•). Each curve begins with the month for which the observed ice cover is used to initiate the calculation. (After Gordon and Taylor, 1975).

BARKLEY 1

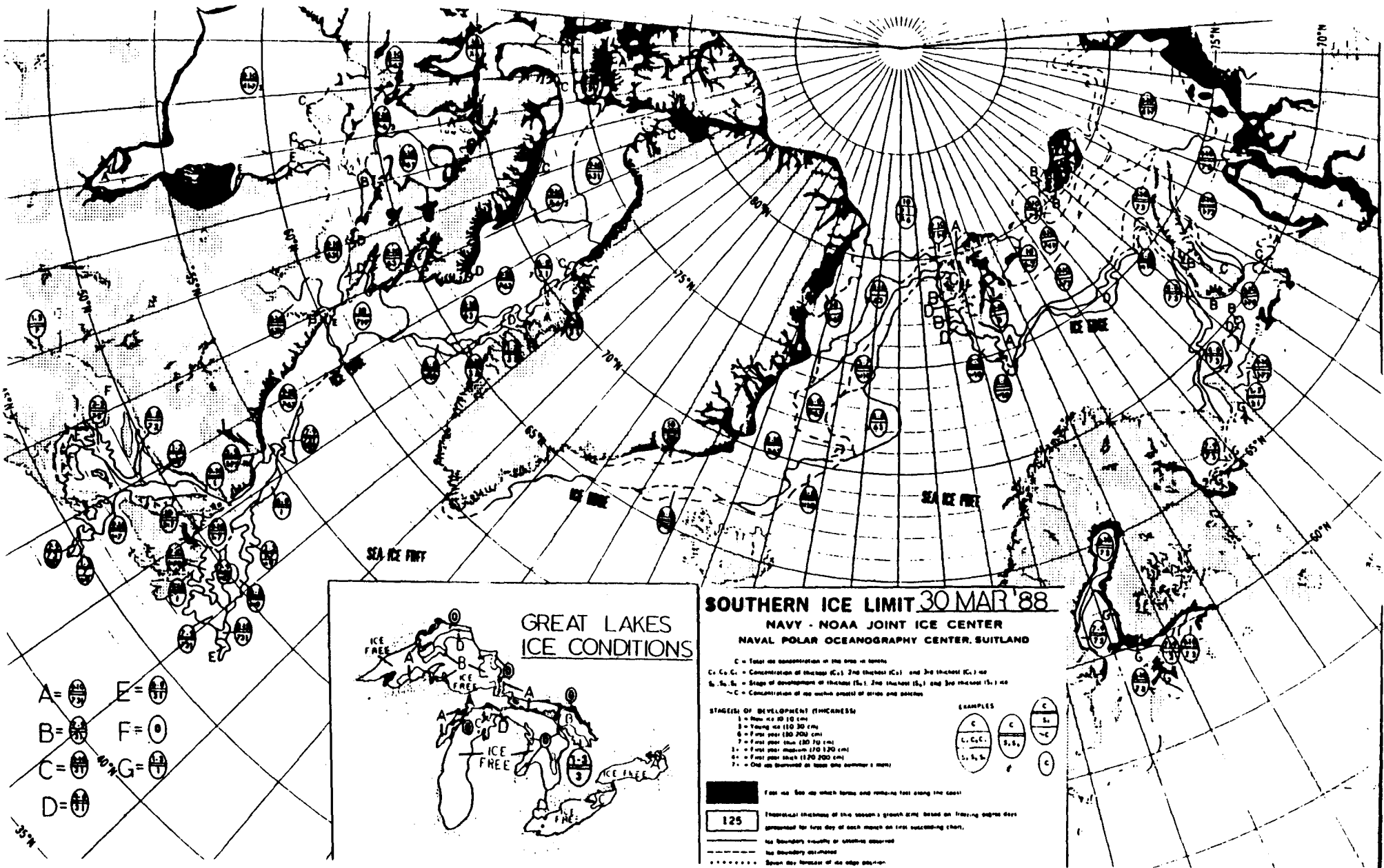


AREA IN 10 6 SQ KM



AREA COVERED BY SEA ICE

MAP OF GREAT LAKES



- A =
- B =
- C =
- D =
- E =
- F =
- G =



SOUTHERN ICE LIMIT 30 MAR '88

NAVY - NOAA JOINT ICE CENTER
NAVAL POLAR OCEANOGRAPHY CENTER, SUITLAND

C = Total ice concentration in the area in tenths
C₁, C₂, C₃ = Concentration of the top (C₁), 2nd thickest (C₂) and 3rd thickest (C₃) ice
S₁, S₂, S₃ = Stage of development of the top (S₁), 2nd thickest (S₂) and 3rd thickest (S₃) ice
- C = Concentration of ice within groups of strips and patches

STAGES OF DEVELOPMENT (THICKNESS)

- 1 = None ice (0-10 cm)
- 2 = Young ice (10-30 cm)
- 3 = First year (30-50 cm)
- 4 = First year (50-70 cm)
- 5 = First year (70-100 cm)
- 6 = First year (100-150 cm)
- 7 = Old ice (over 150 cm)

EXAMPLES

125 For use: See up which forms and retaining fast along the coast
Theoretical thickness of the season's growth curve based on filtering paper discs prepared for first day of each month on first succeeding chart.
--- Ice boundary results of satellite observed
- - - - - Ice boundary estimated
..... Show the forecast of the edge position

TABLE 6. Northern hemisphere sea ice products

Source	Parameter	Region	Temporal Frequency	Chart Scale	Record	Digital Processing	Archive
US Navy, NOAA, Coast Guard, National Ice Center	Ice concentration (oktas)	Eastern and Western Arctic	Weekly Chart	1:11.6 Million	1972–present	NCDC	NSIDC ¹
NASA: Nimbus 5 ESMR	Total ice concentration, FYI and MYI fractions	Northern Hemisphere	3-d averages	~50 km resolution	1973–1976	NASA	NSIDC
NASA: Nimbus 7 SMMR	Total ice concentration, FYI and MYI fractions	Northern Hemisphere	3-d averages	~ 50 km resolution	1978–1987	NASA	NSIDC
DMSP: SSM/I	Total ice concentration, FYI and MYI fractions	Northern Hemisphere	Daily	~25 km resolution	1987–present	NSIDC	NSIDC

¹A catalogue describing these and other products archived and distributed by NSIDC is available.

TABLE 7. Canadian sea ice charts

Title	Parameters	Region	Temporal Frequency	Chart Scale	Record	Archive
Composite ice charts	Ice concentration, (tenths) ice type/age, ice floe size, leads, for the date of issue.	Eastern seaboard	2-7d (Dec-July)	1:4 Million	1969-present	AES (microfiche)
		Hudson Bay	7d (June-Nov) 30d (Dec-May)		1971-present	1975-82 (digital)
		Eastern Arctic and Western Arctic	7d (June-Nov); 30d (Dec-May)		1968-present	1975-80 (digital)
		Great Lakes	7d (Dec-May)		1969-present	
Historical ice charts	Ice concentration, (tenths) ice type/age, ice floe size, leads, for the date of issue.	North of 65°N	7-d (May-Oct)	1:6.25 Million	1959-1974	AES (digital data base) Replaced by composite ice charts
		Eastern seaboard, Hudson Bay, Foxe Basin	7-d (Dec-May)			
Current ice conditions	Ice concentration, (tenths) ice type/age, ice floe size, leads, for the date of issue.	16 areas 1:2 Million scale	Daily for marine operational seasons from 1964 Arctic-breakup to freeze-up	1:1 to 1:2 Million	1956-present	AES (microfilm)

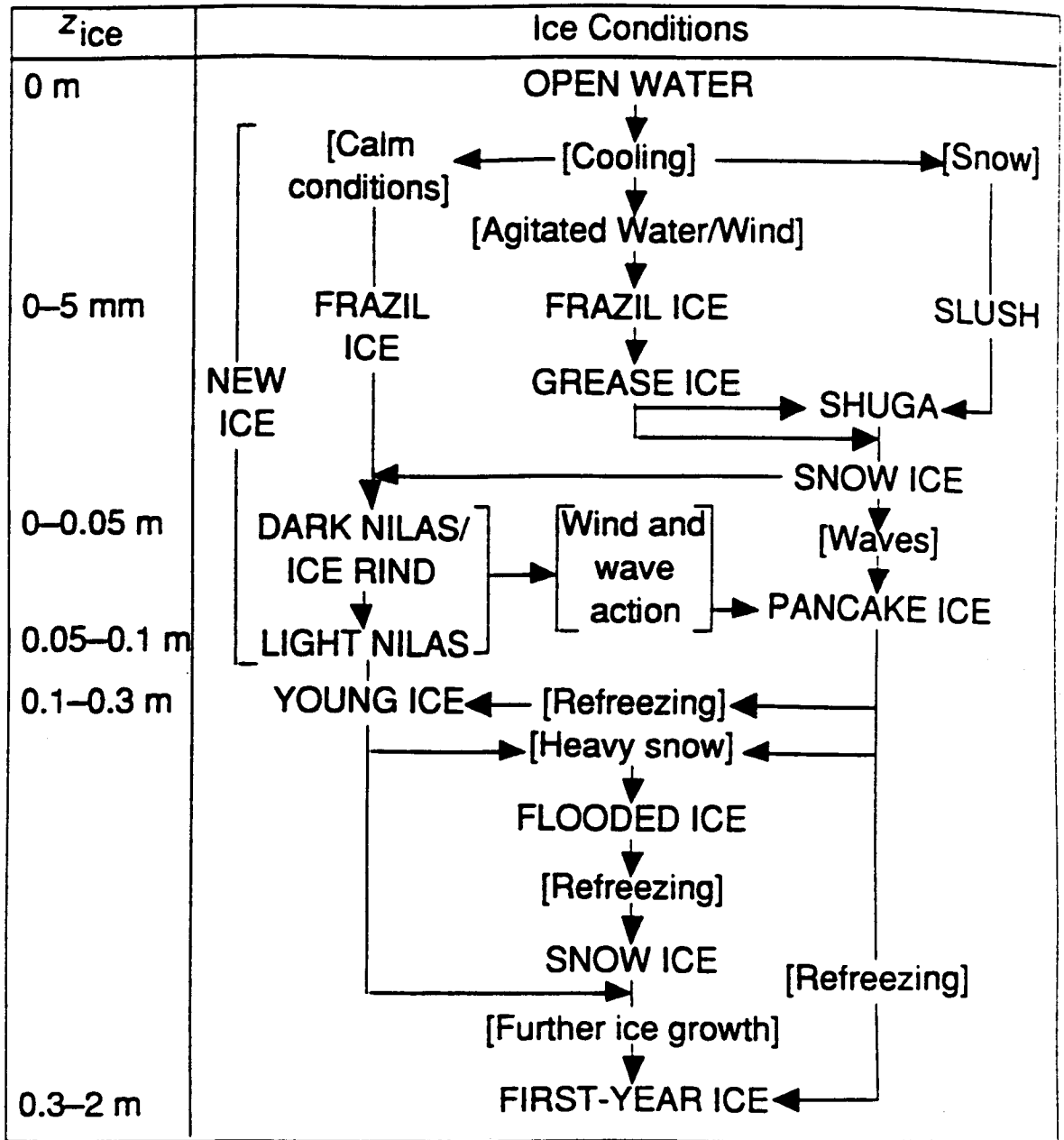


Fig. 14-1. Evolutionary sequence for thin sea ice. Ice types are shown in capital letters and related environmental processes are enclosed in square brackets.

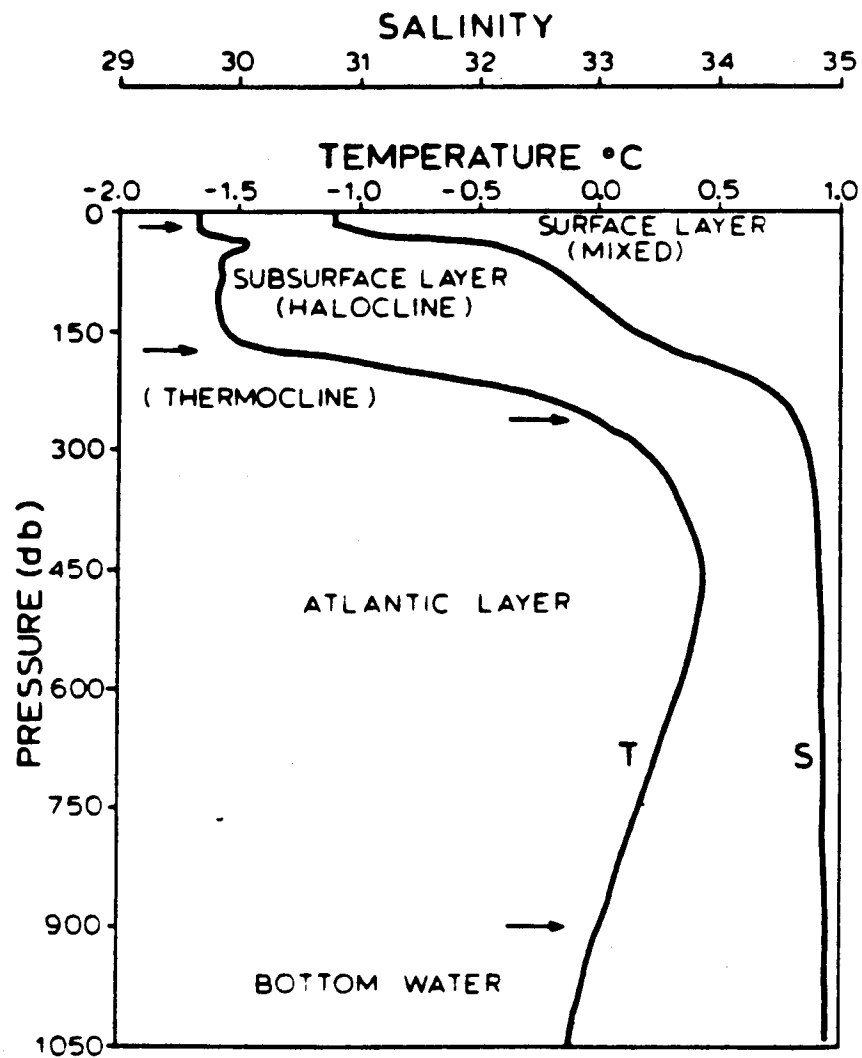


Fig. 1. Typical hydrographic profiles in the Canadian Basin of the Arctic Ocean, illustrating the principal water masses (FSRG data, 1981).

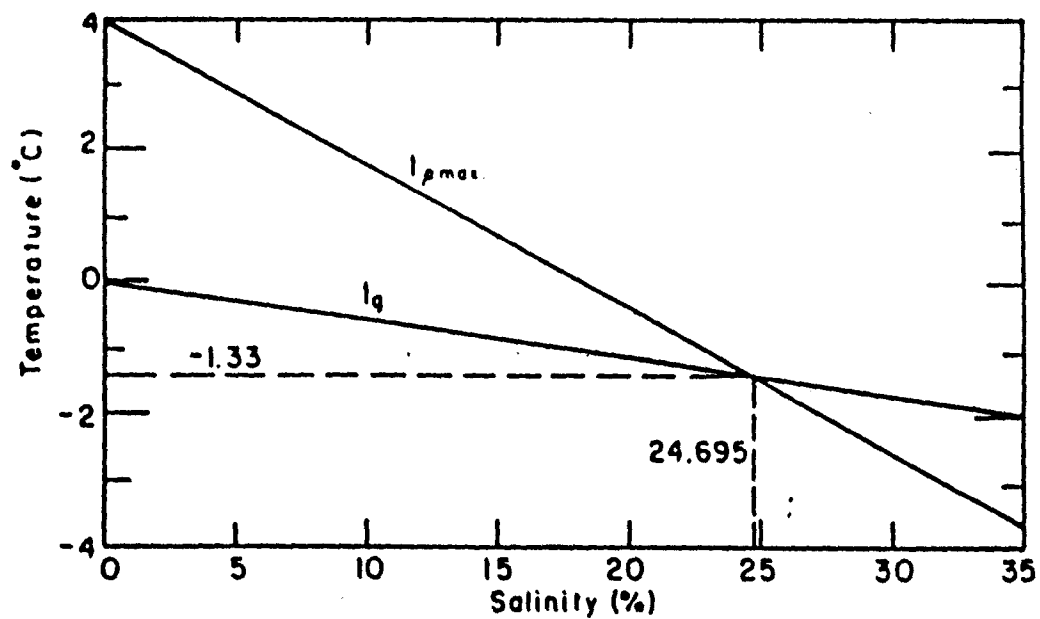


Fig. 7. Temperature of the density maximum t_{max} and of the freezing point t_g for seawater of different salinities.

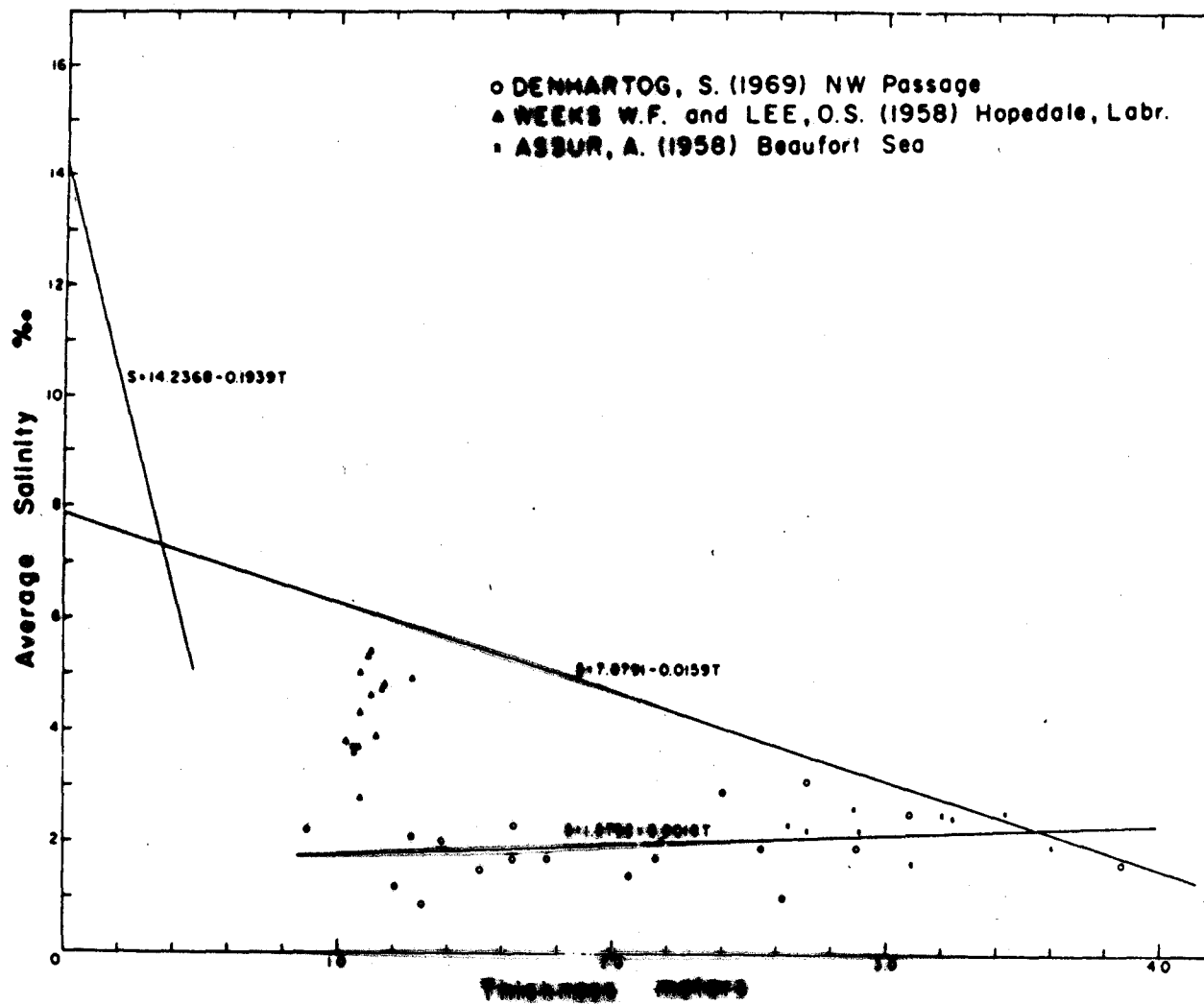


Fig. 67. Average salinity of sea ice as a function of ice thickness for warm sea ice sampled during the end of the melt season (Cox and Weeks, 1975).

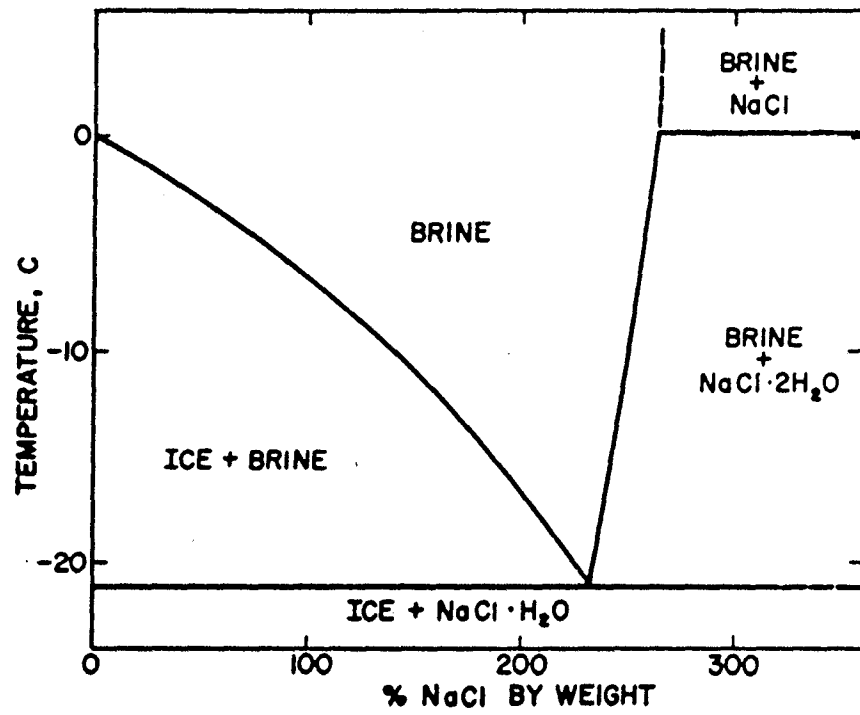


Fig. 2. A portion of the phase diagram NaCl-H₂O.

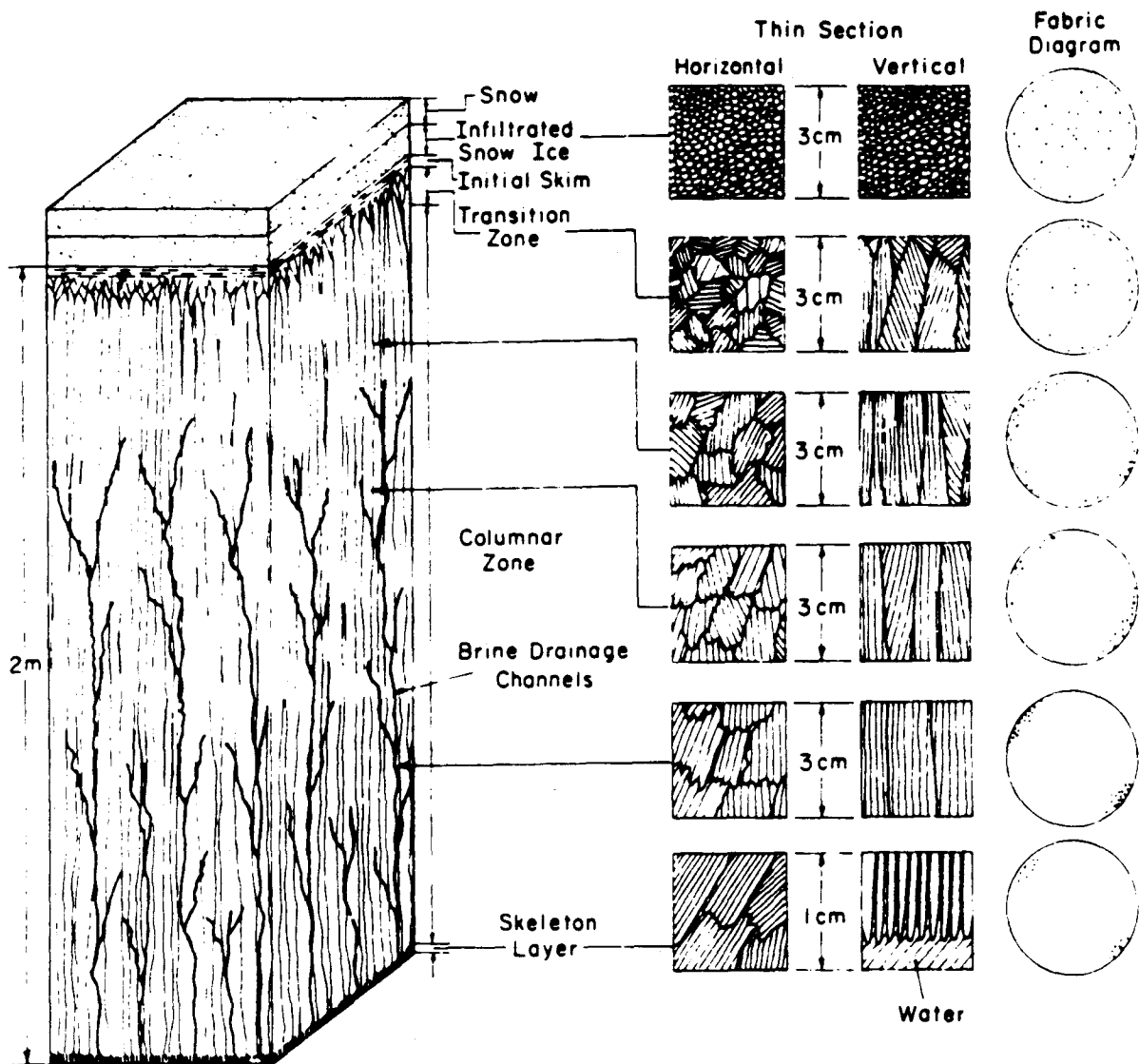


Figure 2.20 Schematic depicting major structural, crystal texture, and *c*-axis fabric elements in a 2-m-thick first-year sea ice sheet. In this schematic the initial skim of frazil ice is overlain in succession by snow ice and snow. The skeleton layer at the bottom of the sheet corresponds to the region of dendritic ice growth. Adapted from Schwarz and Weeks (1977); courtesy of the International Glaciological Society.

Sea Ice Growth Relations
(see Maykut 1986)

Heat flux thro' ice balanced by latent heat due to freezing

$$\int -K_i T_s / Z dt = L_f \partial M / \partial t = \int L_f \rho_i dZ \quad \leftarrow \text{ice thickness change}$$

K_i = thermal conductivity of ice M = ice mass

Z = ice thickness t = time

T_s = surface temperature ρ_i = ice density

By integration: $Z^2 = (-2T_s \cdot K_i \cdot t) / (L_f \cdot \rho_i)$ (if $Z = 0$, at $t = 0$)

JACOBS (INSTAAR Paper #9)

Flux at ice surface = $[T_A - T_W] / [(Z/K_i) + (h/K_s)]$ T_A = air temperature

h = snow depth

T_W = water temperature

Balanced by

$$L_f \rho_i \Delta Z / \Delta t \quad + \quad H_i \cdot Z \quad + \quad F_w$$

Lat. Heat release Heat content Water transport
by freezing of ice (current)

$$\text{Growth Rate} \quad \Delta Z / \Delta t = 1 / L_f \rho_i [T_A - T_W] / [(z/K_i) + (h/K_s)] - H_i \cdot Z - F_w$$

$$[H_i = \rho_i (T_2 - T_1) (0.5 + 4.1S / T_1 T_2) ; S = \text{salinity ppm}]$$

↑
Heat required to raise T from T_1 to T_2

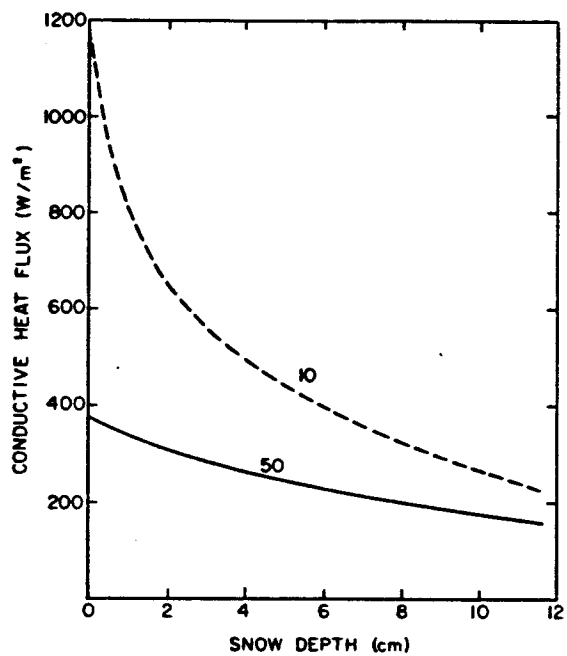


Fig. 10. Effects of snow depth on heat conduction in young ice during mid-winter ($T_a = -34^\circ\text{C}$). The dashed curve shows 10 cm thick ice and the solid curve 50 cm thick ice.

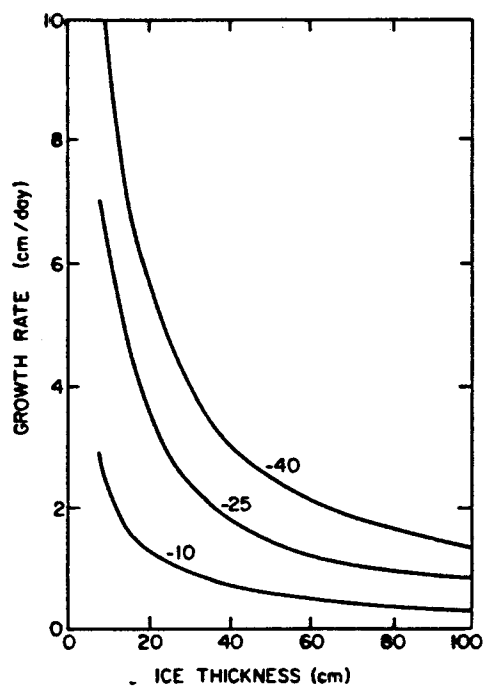


Fig. 15. Dependence of growth rates in young sea ice on thickness for air temperatures of -10 , -25 , and -40°C .

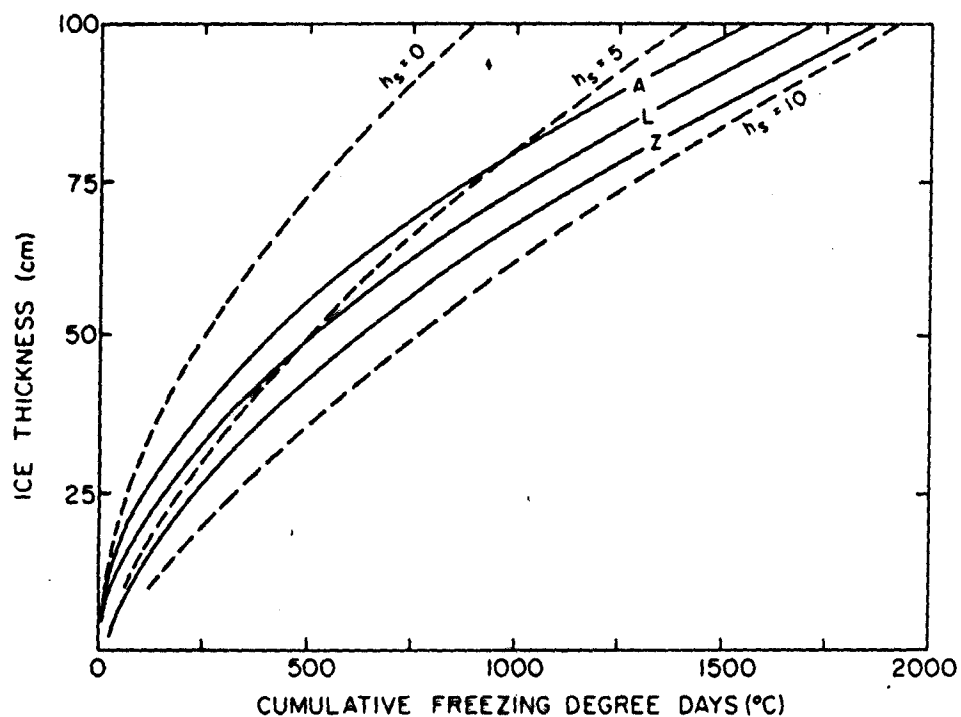


Fig. 14. The solid curves show ice growth predictions by the empirical formulas of Anderson (A), Lebedev (L), and Zubov (Z). Dashed curves show theoretical relationships between ice thickness and degree-days obtained from eq. (5.23) for different thicknesses (h_s) of snow.

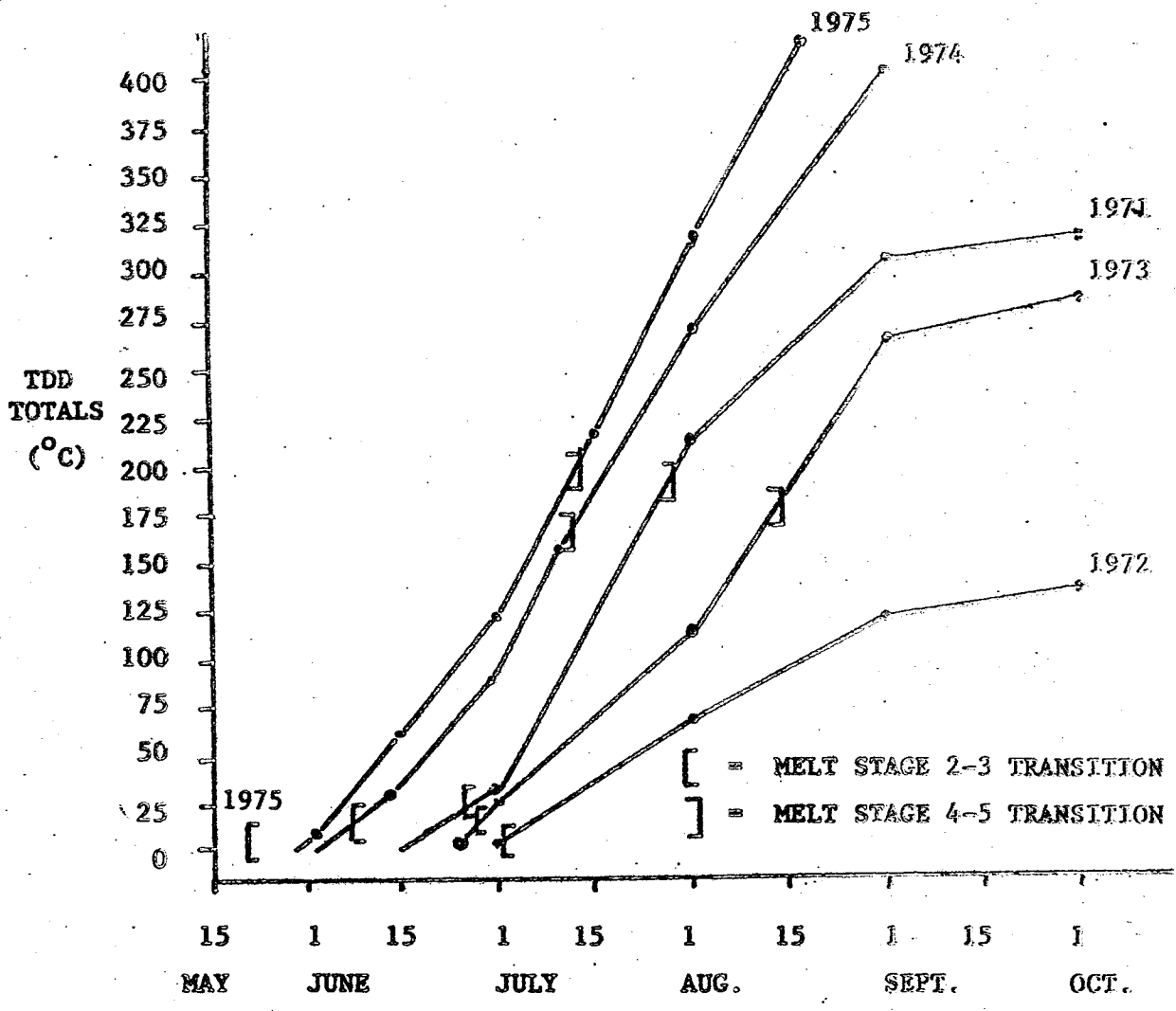
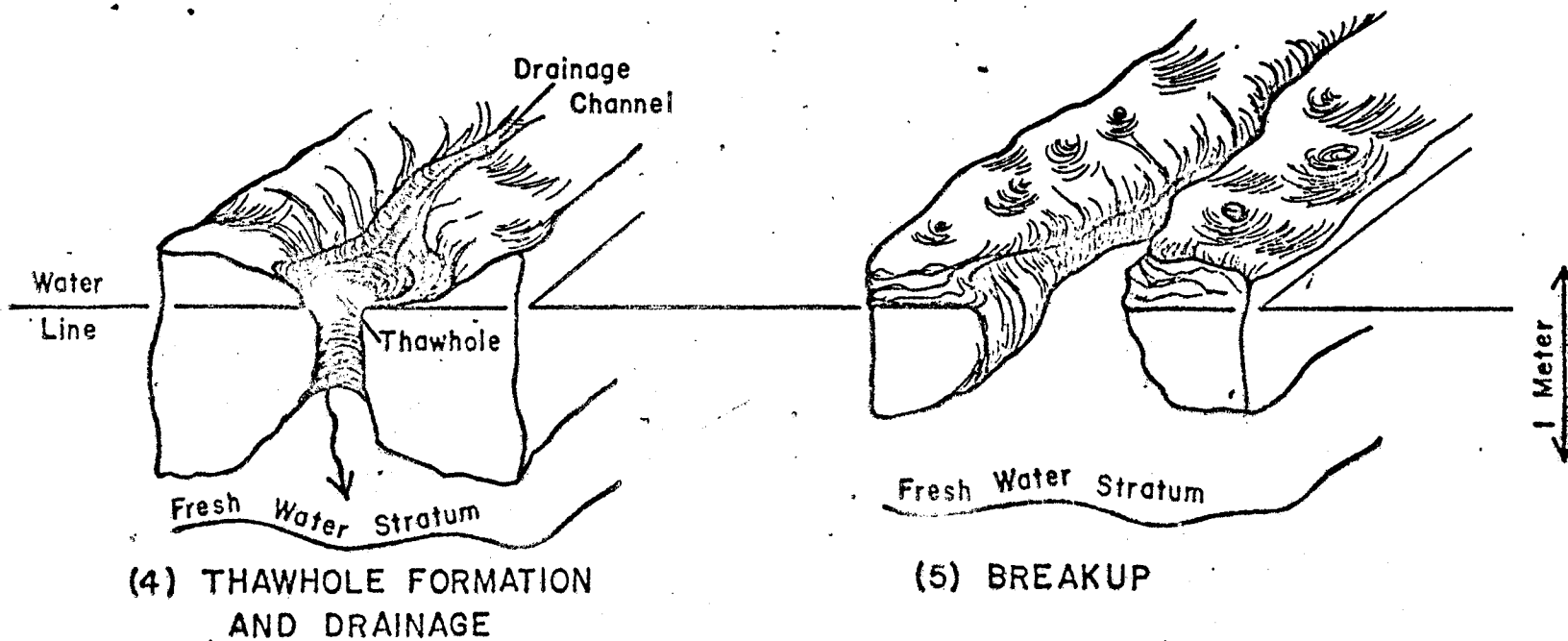
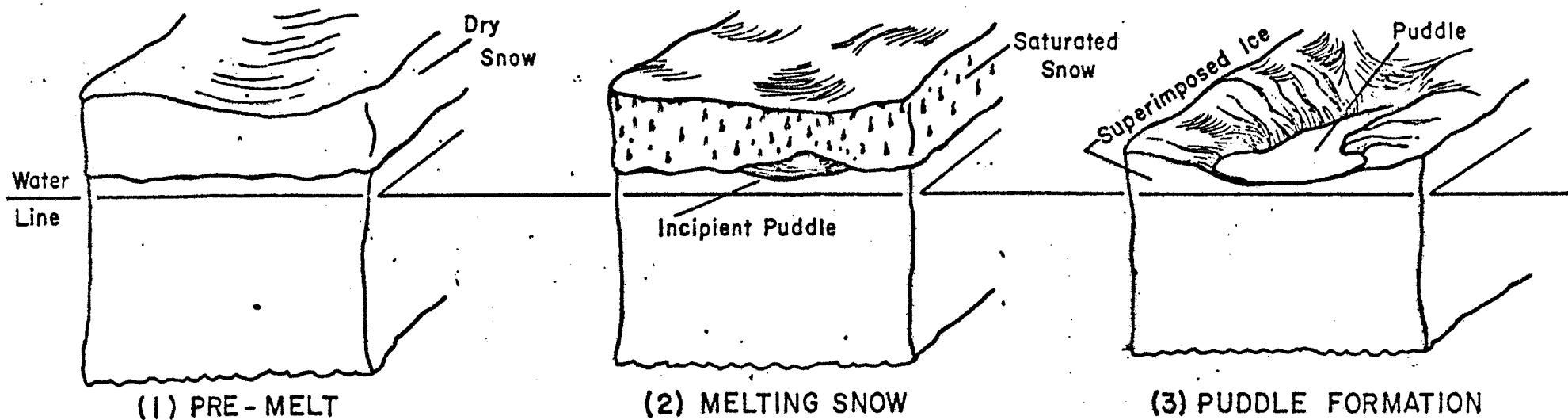
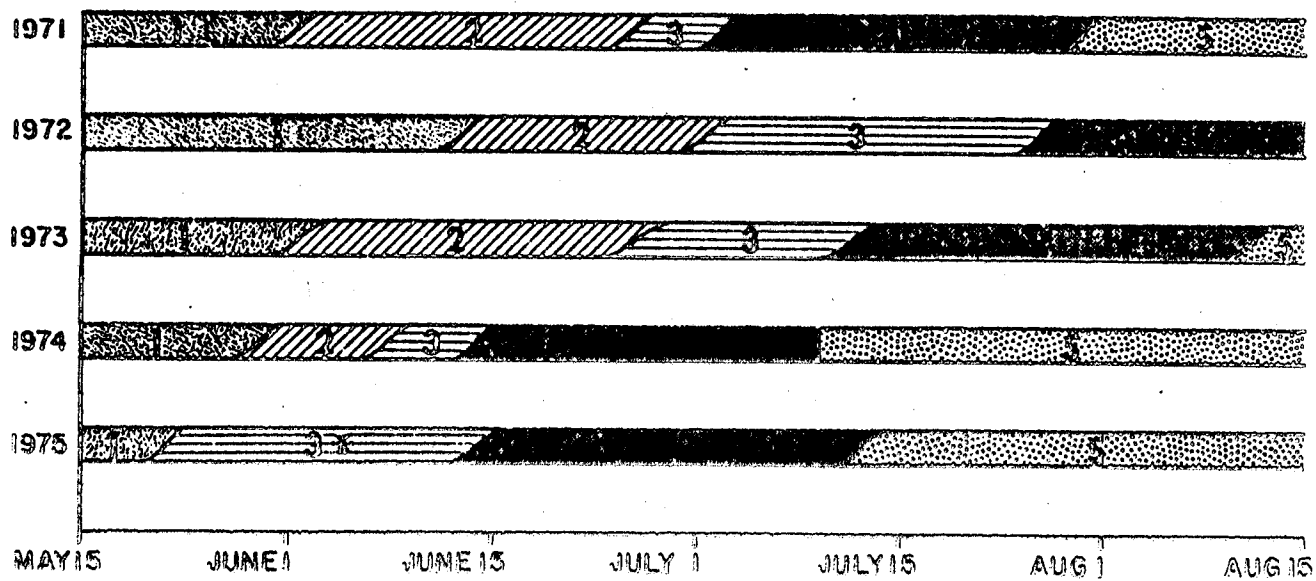


Figure 7.1

Thawing degree - day totals (°C) at Broughton Island (581 a.s.l.) in summers 1971-75. Melt stage transitions 2-3 and 4-5 (breakup) are also shown.





* Very low snowfall in 1975 did not allow stage 2 formation

APPROXIMATE TRANSITION DATES FOR MELT STAGES IN THE BROUGHTON ISLAND VICINITY

Figure 5.B. 9. The progression of the melt stages, on the fast ice at Broughton Island 1971-75.

CONTROLS ON ANNUAL ICE GROWTH/DECAY

SNOW COVER —

PRECIPITATION SYSTEM

SNOWFALL ↗

↘

FREEZING LEVEL

SNOW MELT — SOLAR ENERGY ABSORPTION
WARM AIR MASSES

SEA ICE — BULK FREEZING AT/NEAR SURFACE

— (SNOW COVER-INSULATION)

— ARCTIC FRESHWATER LAYER

— ICE MOTION DUE TO WIND → OPENINGS RIDGES

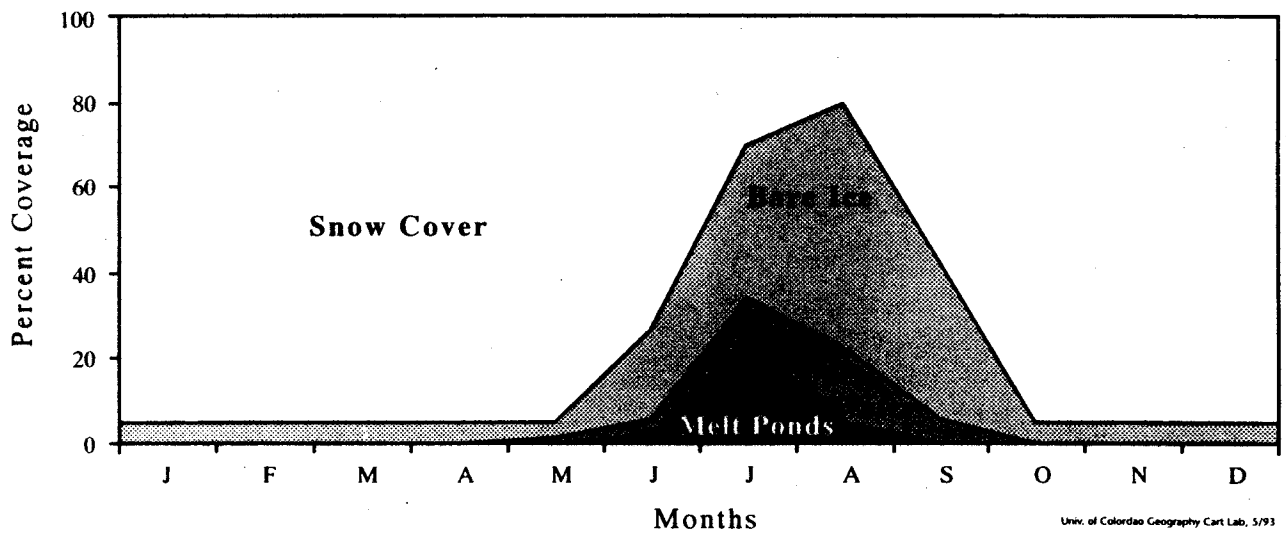
DECAY — BY ENERGY ABSORPTION

— ICE EXPORT BY OCEAN CURRENTS/WIND

ARCTIC ICE AVERAGES 3.5 m THICK

ANTARCTIC ICE ~ 1 m THICK

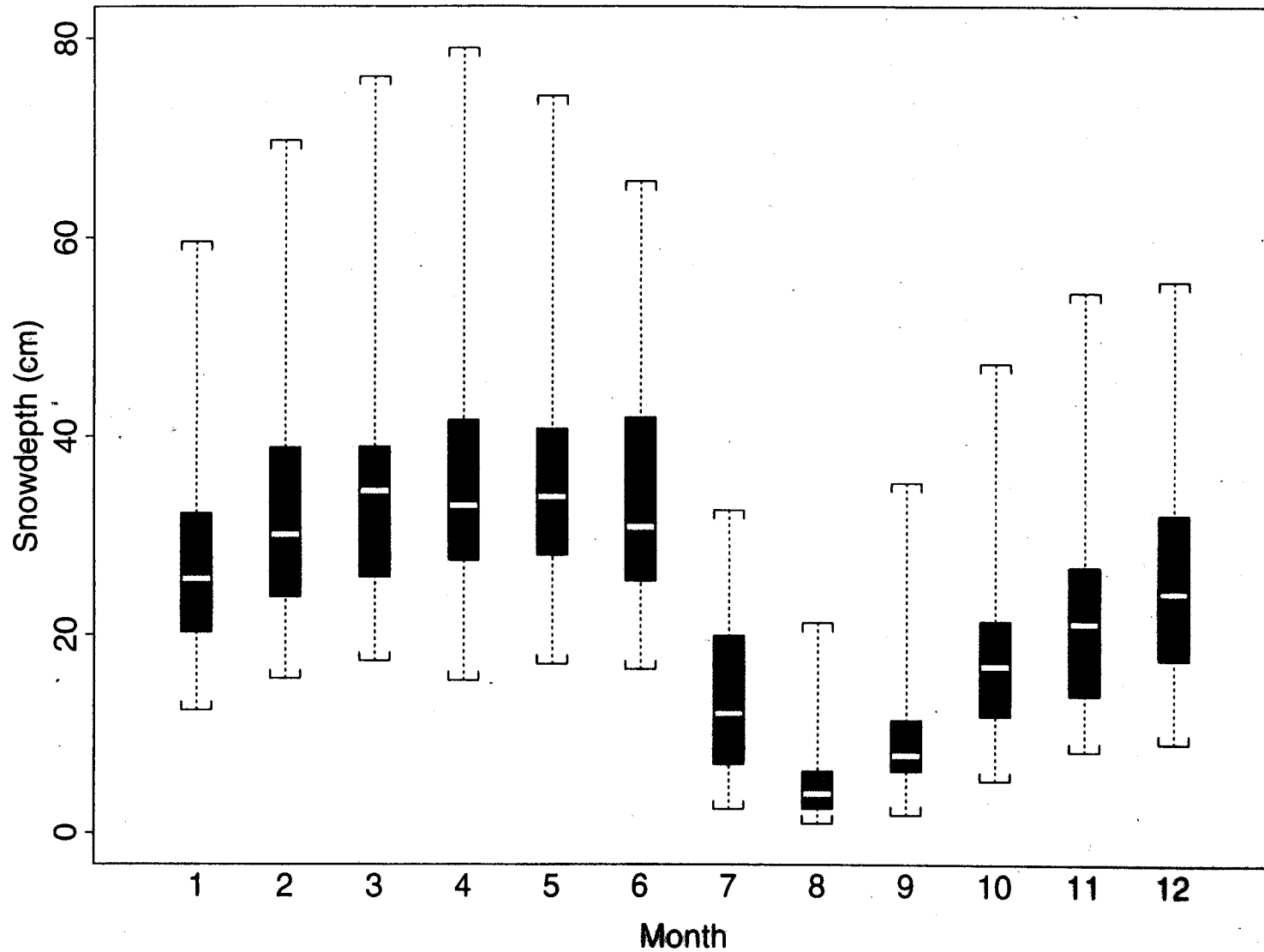
~ 15% OF ARCTIC ICE AREA EXPORTED ANNUALLY



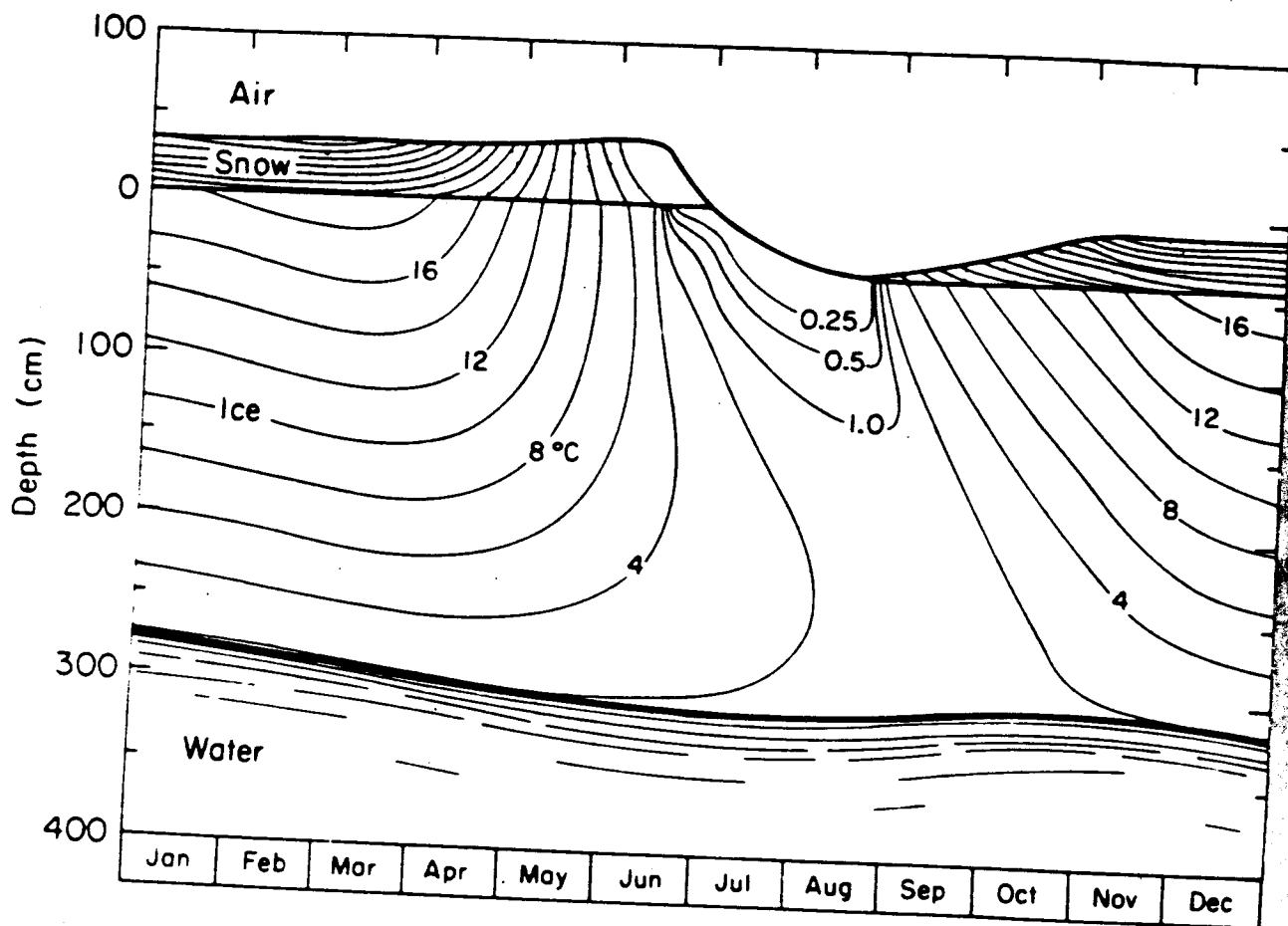
Approximate Seasonal Course of Average Fractional Cover of Surface Types in the Central Arctic

COADS DATA (M. CLARK)

Snow depth from Arctic drifting stations (1954-1991)



Sea Ice Growth, Drift, and Decay



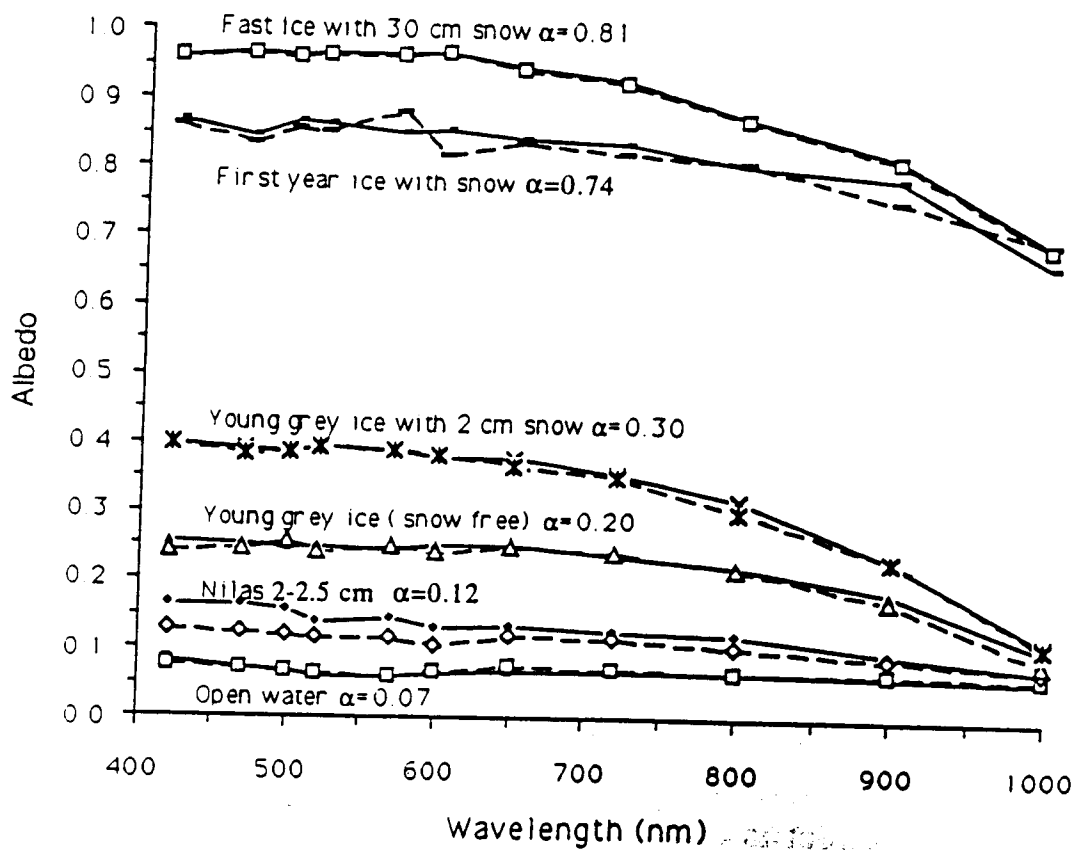


Figure 2 Measured spectral albedos versus wavelength (nm) for different types of Antarctic sea ice. Source: From Allison *et al.* (1993) with corrections. Two sets of measurements are plotted for each type and also the calculated all-wave albedo

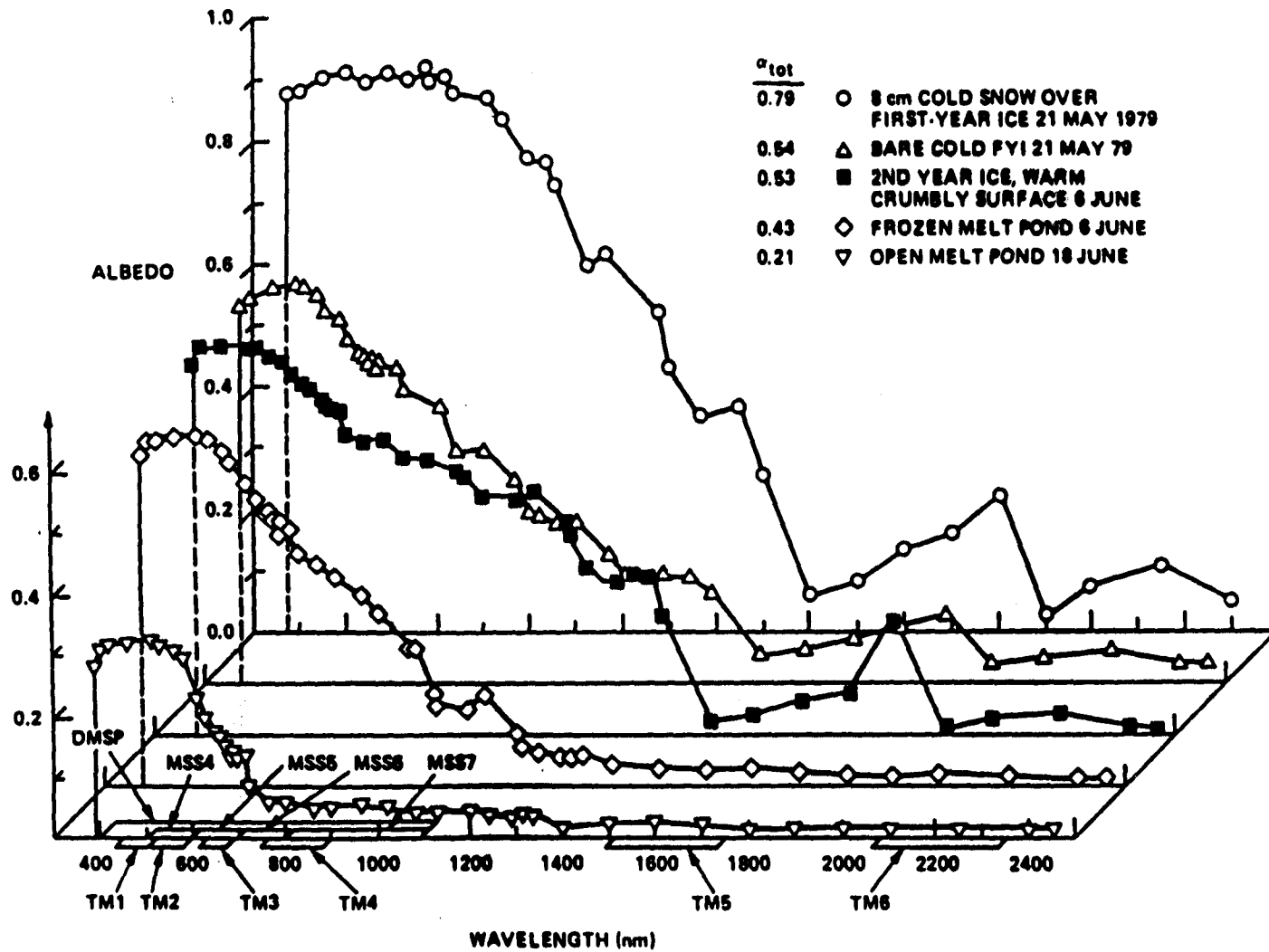


Figure 3.2 Sea ice albedos collected by Dr Tom Grenfell (University of Washington) near Barrow, Beaufort Sea. These values represent samples as no effort has been made to generalise by season or region. Some satellite sensor bands are shown (ie LANDSAT MSS and TM). From Carsey and Zwally (1986).

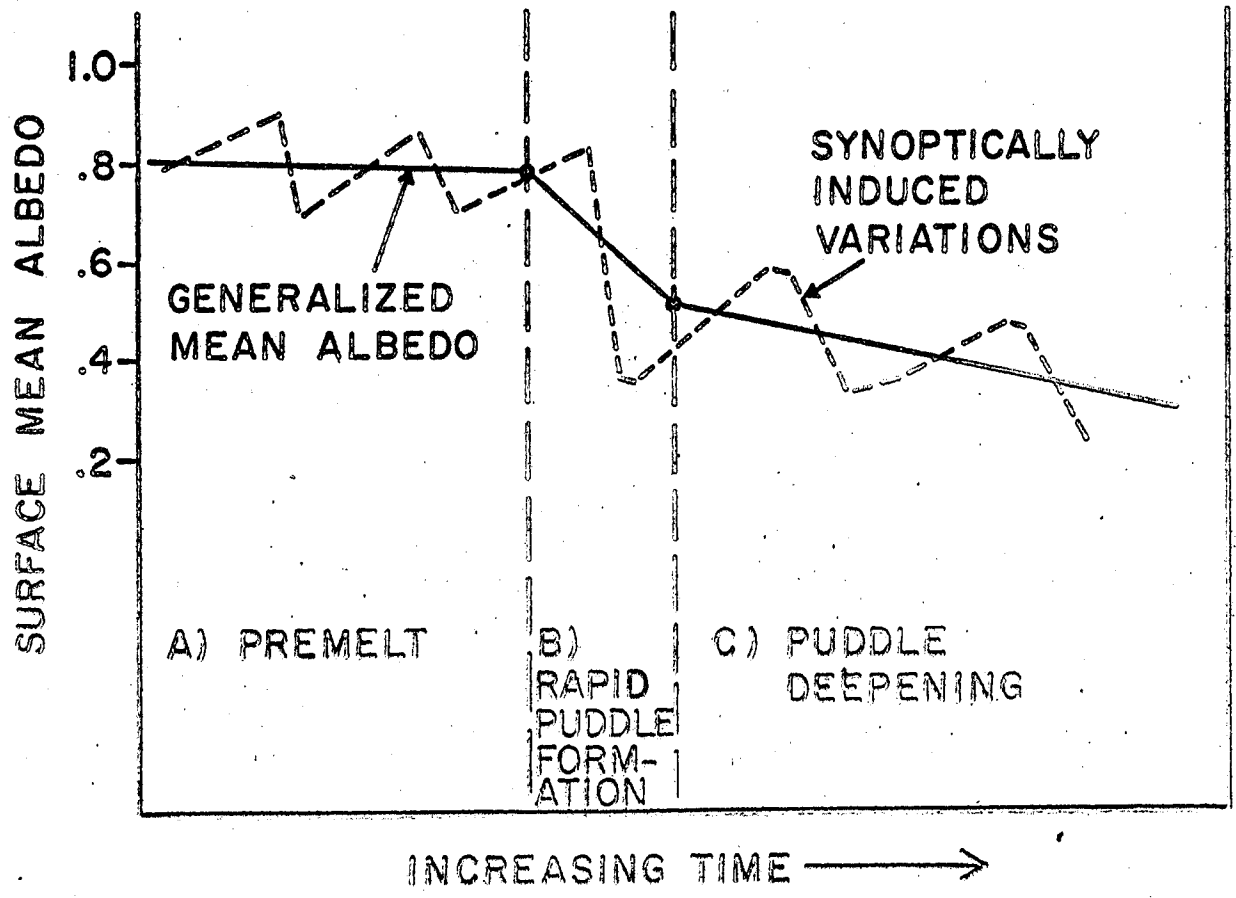
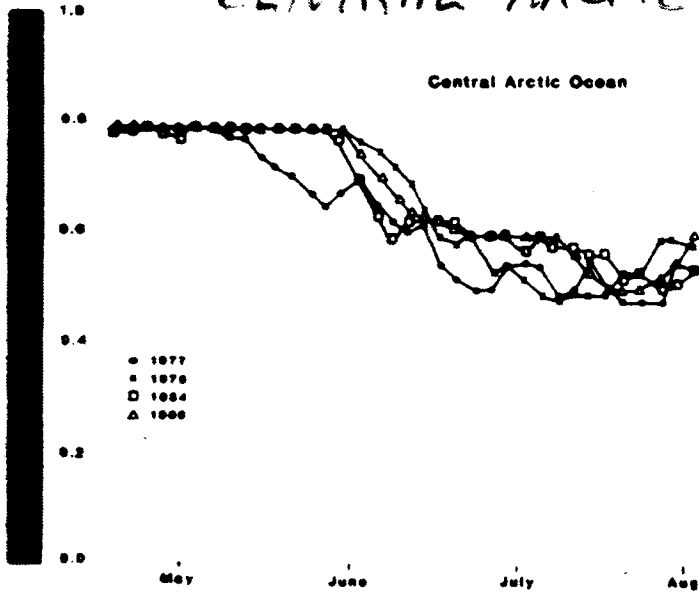


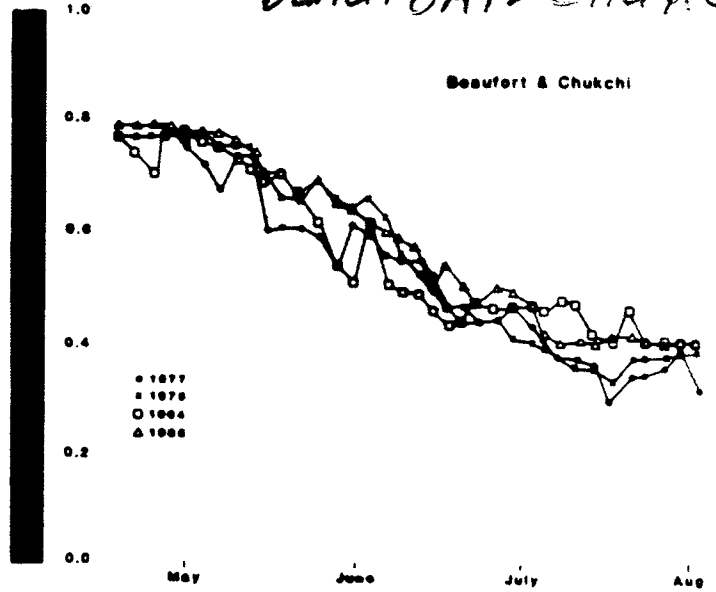
Figure 68. 5. Schematic outline of the trend of fast ice albedo during the summer decay season.

CHANGES IN ALBEDO BY STUDY REGION

CENTRAL ARCTIC

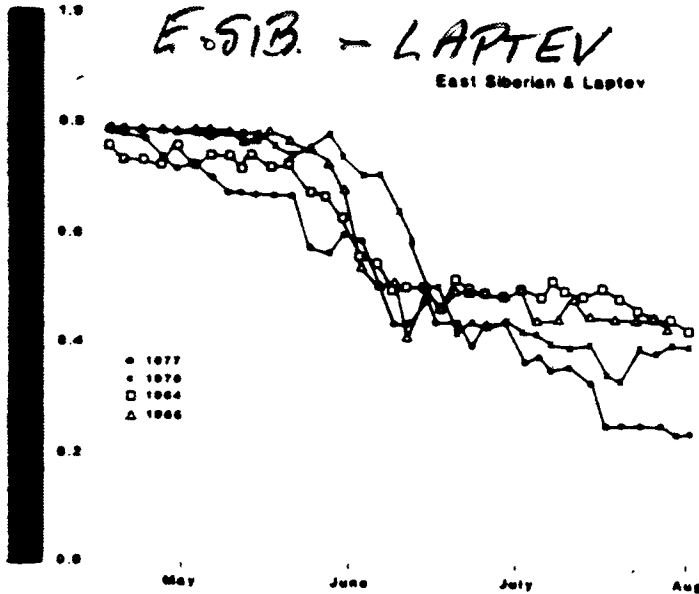


BEAUFORT-CHUKCHI



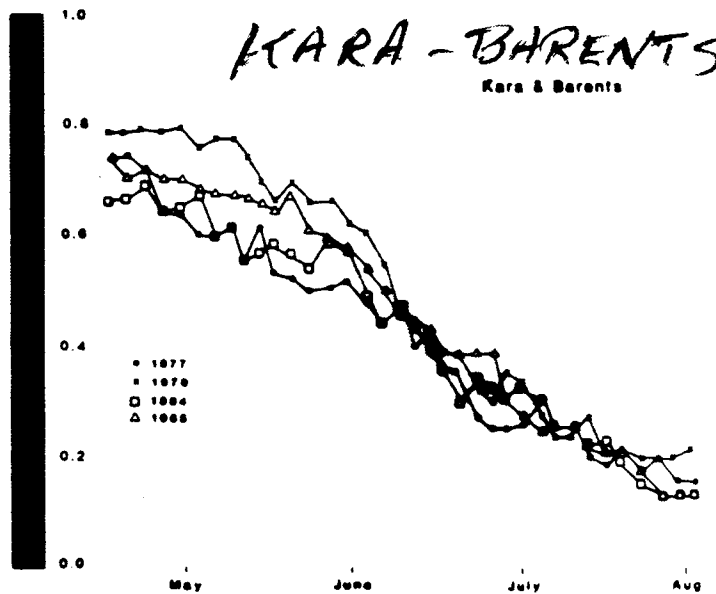
E. SIB. - LAPTEV

East Siberian & Laptev



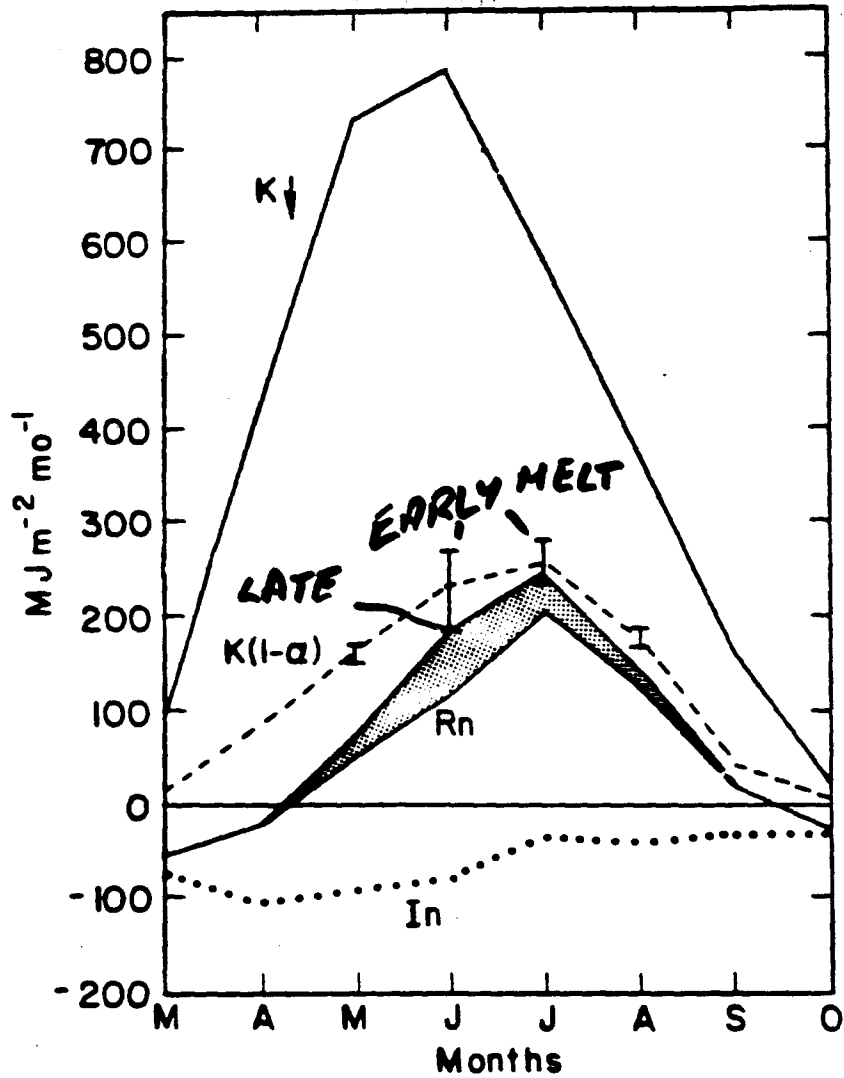
KARA-BARENTS

Kara & Barents

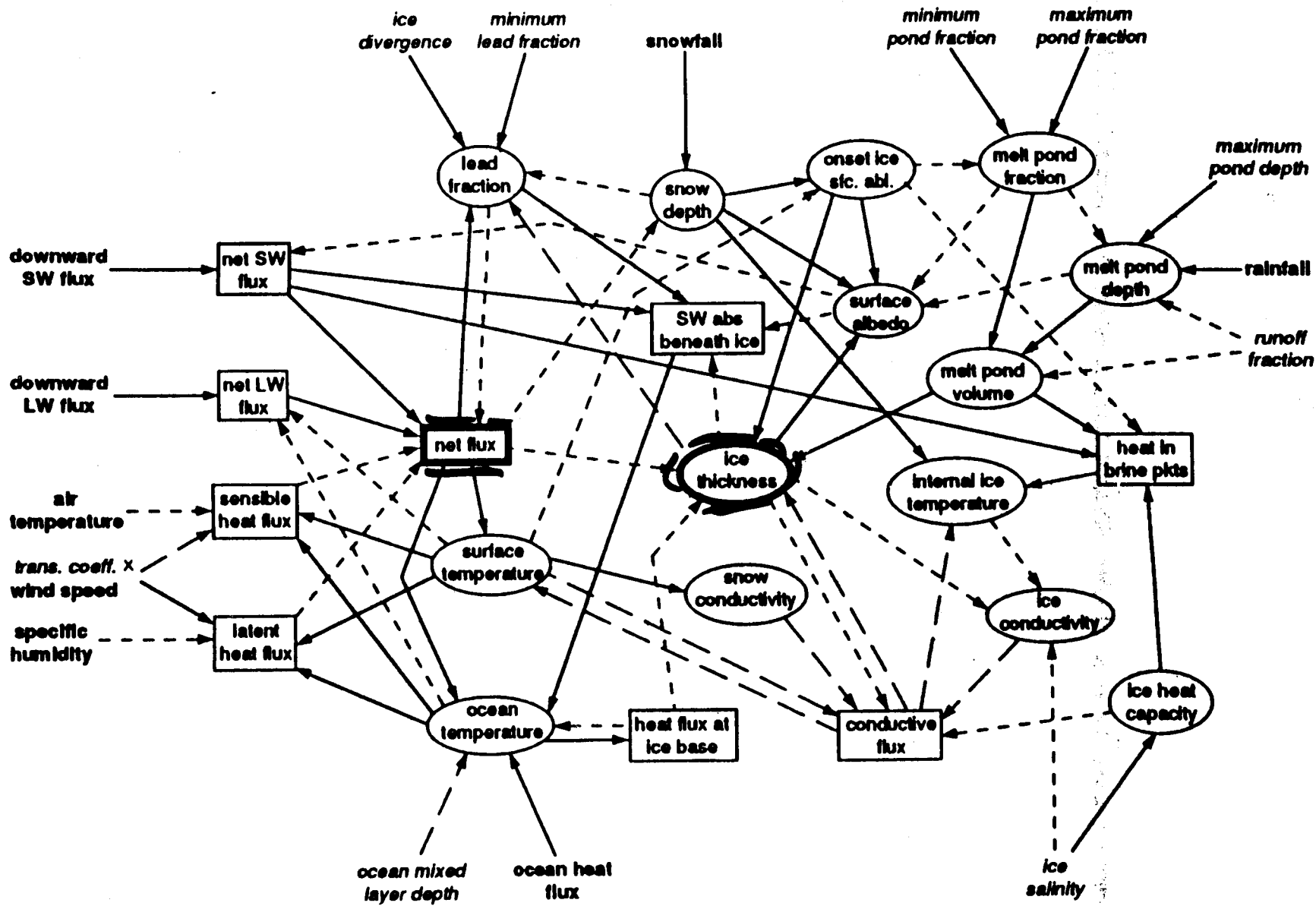


M J J A

M J J A



Barry et al 1989.



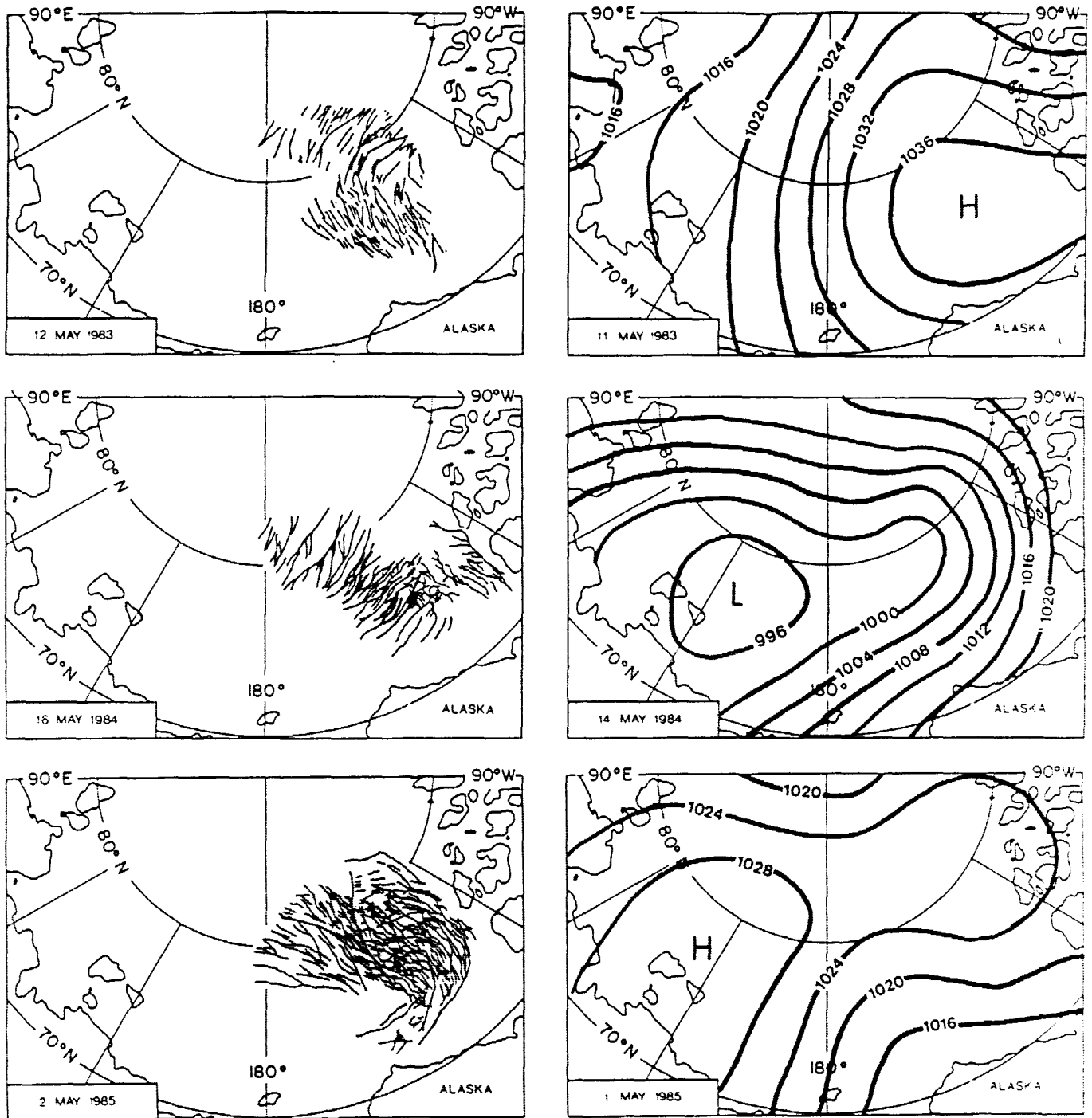
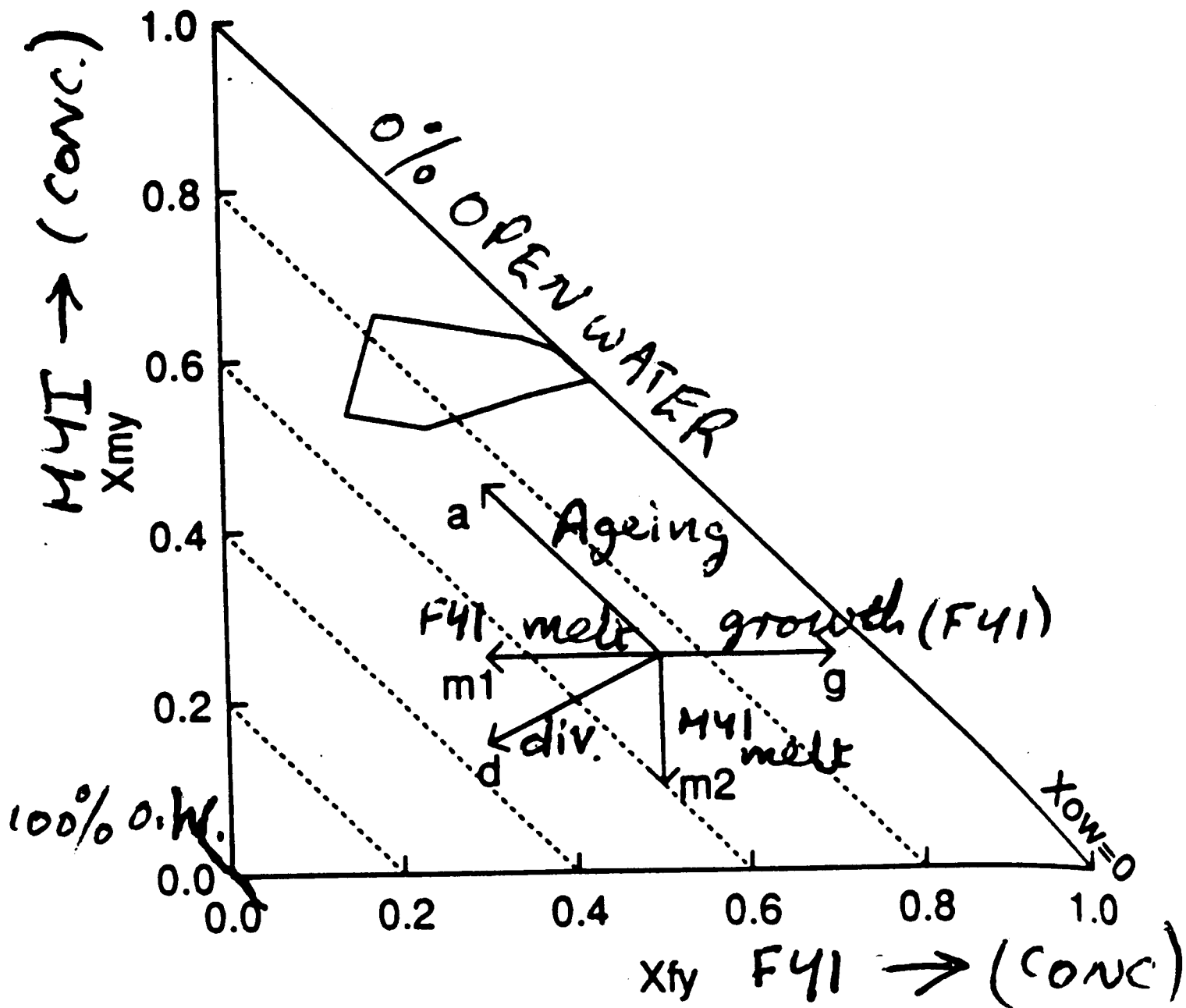
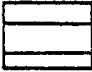




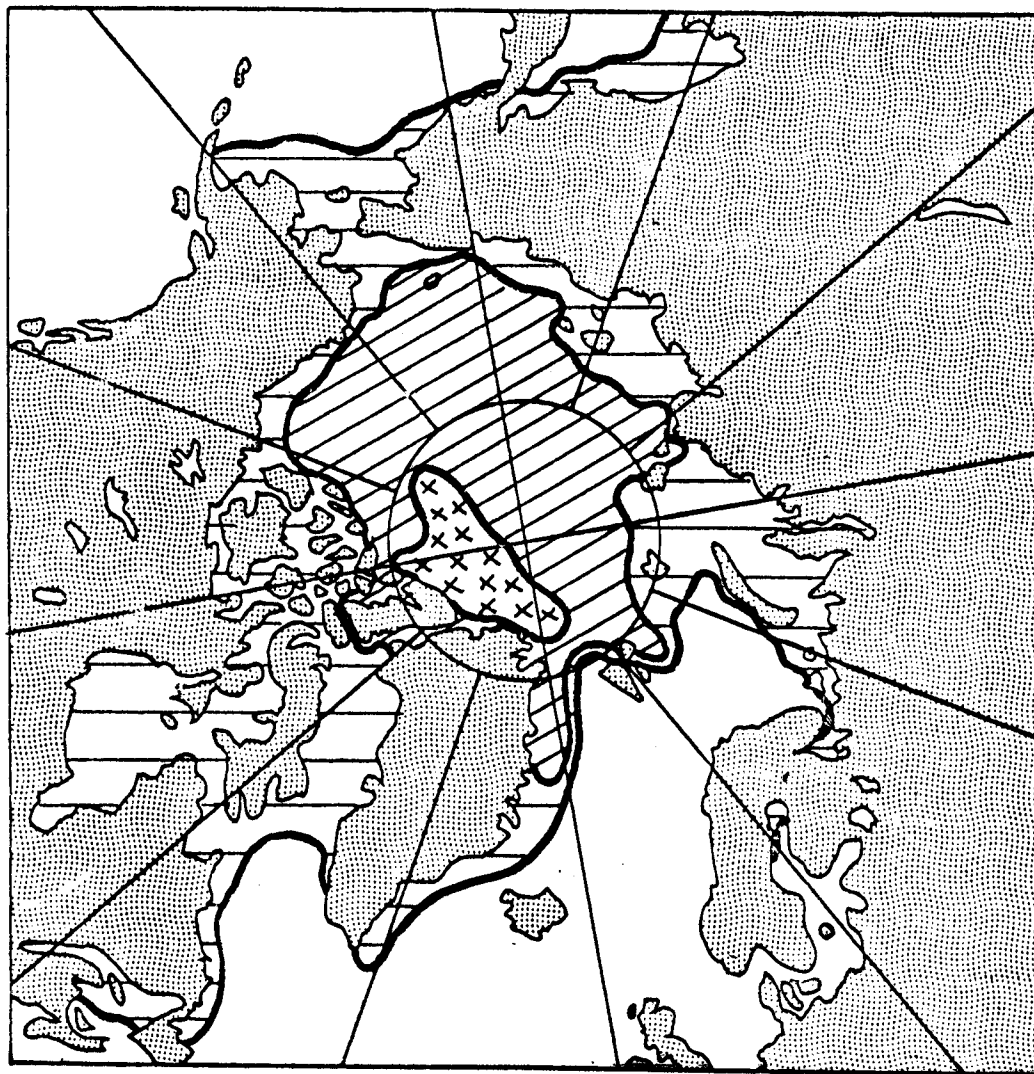
Fig. 2. Lead patterns and corresponding mean sea-level pressure (mbar) patterns in the Beaufort Sea in May of three successive years: (a) 1983; (b) 1984; (c) 1985.

Ротнрок & Томас, 1990


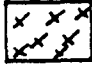
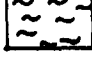


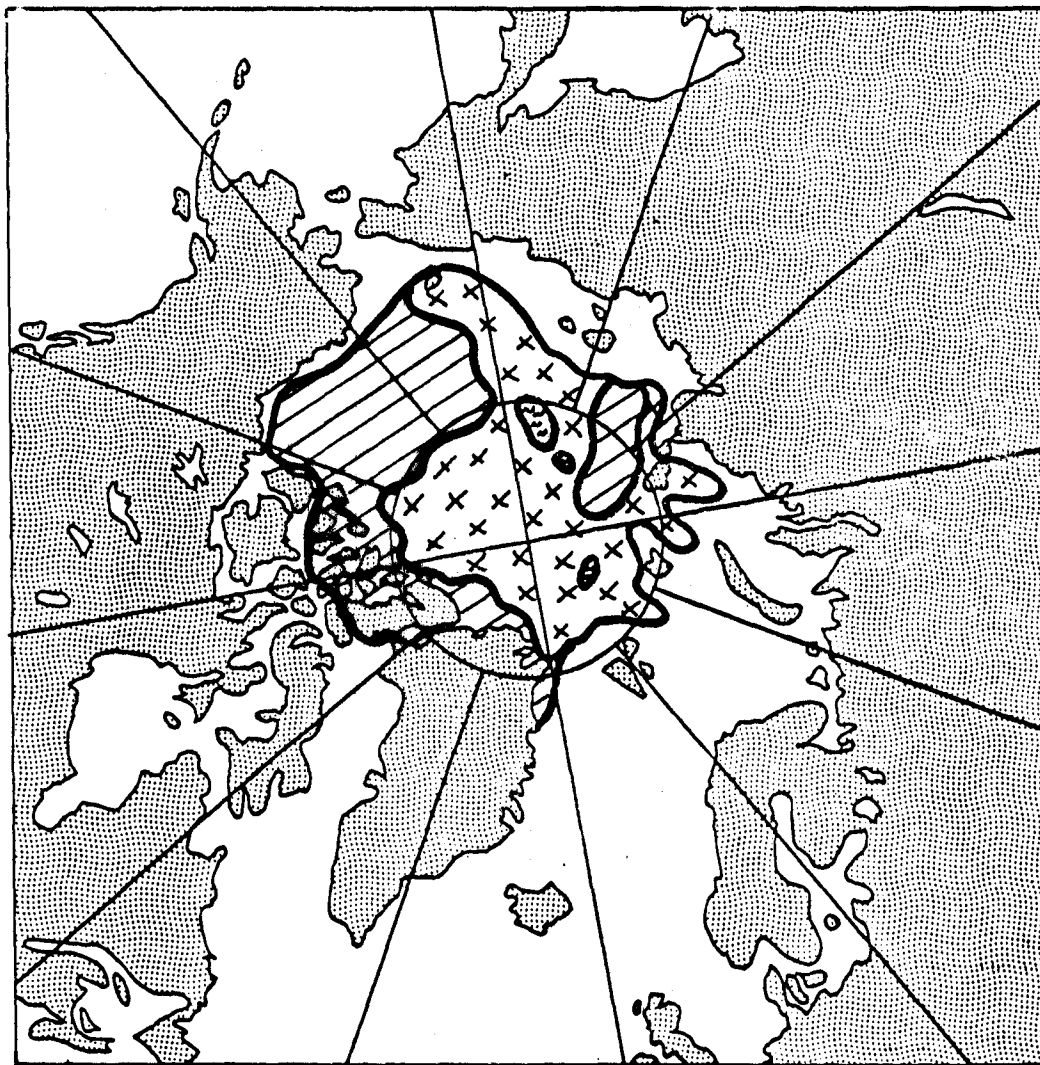
ICE TYPES / ICE BOUNDARIES FOR MAXIMUM EXTENT, 1974
(As at Feb. 27 - March 2)

-  Mainly young (first yr) sea ice
-  Mixed multiyear and first-year sea ice
-  Thick multiyear pack ice



ICE CONCENTRATIONS / ICE BOUNDARIES FOR MINIMUM EXTENT, 1974
(As at September 4 and 7, 1974)

-  Low ice concentration (multiyear)
-  Dense ice concentration (multiyear)
-  Polynya / very low ice concentrations



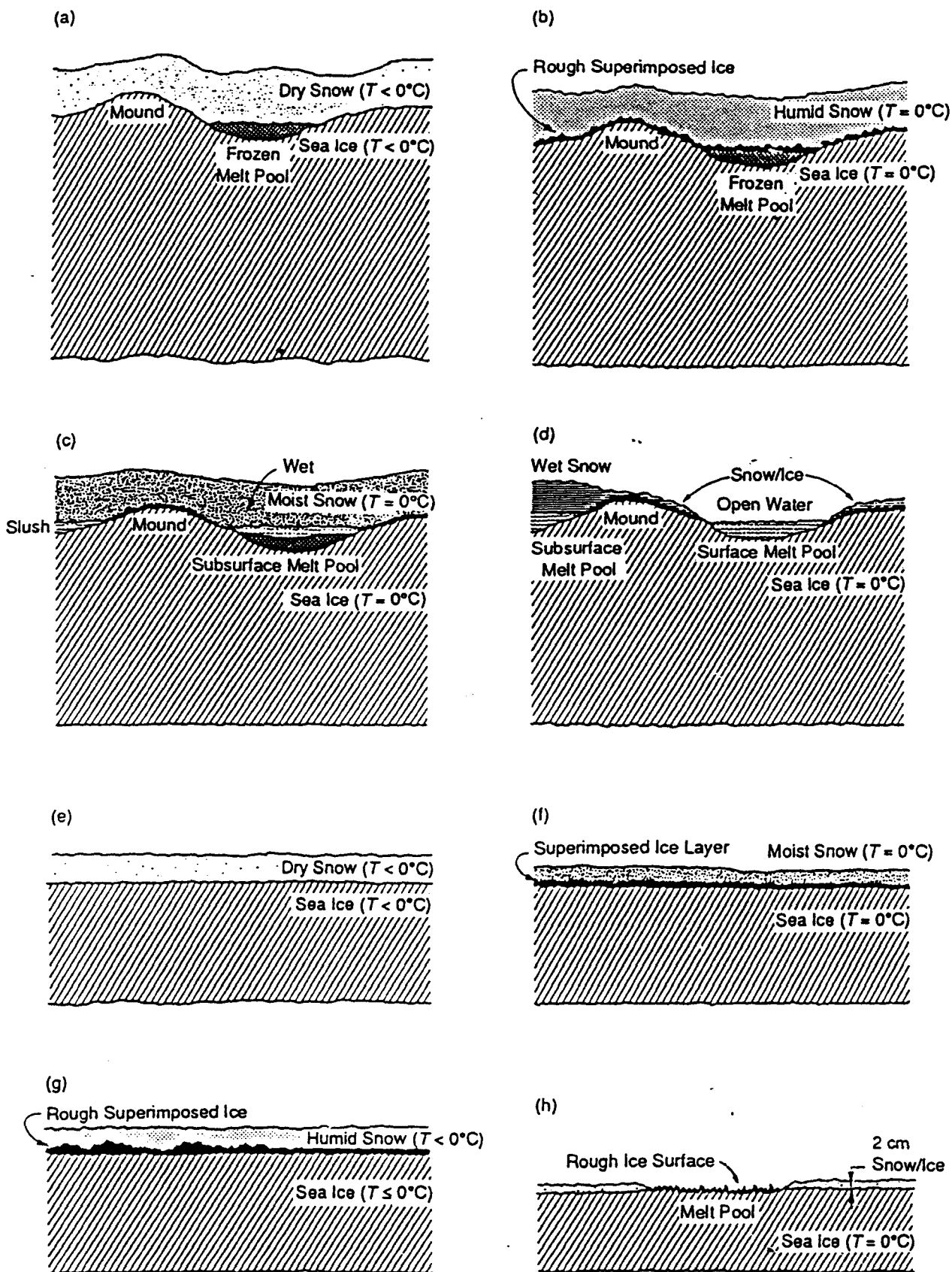
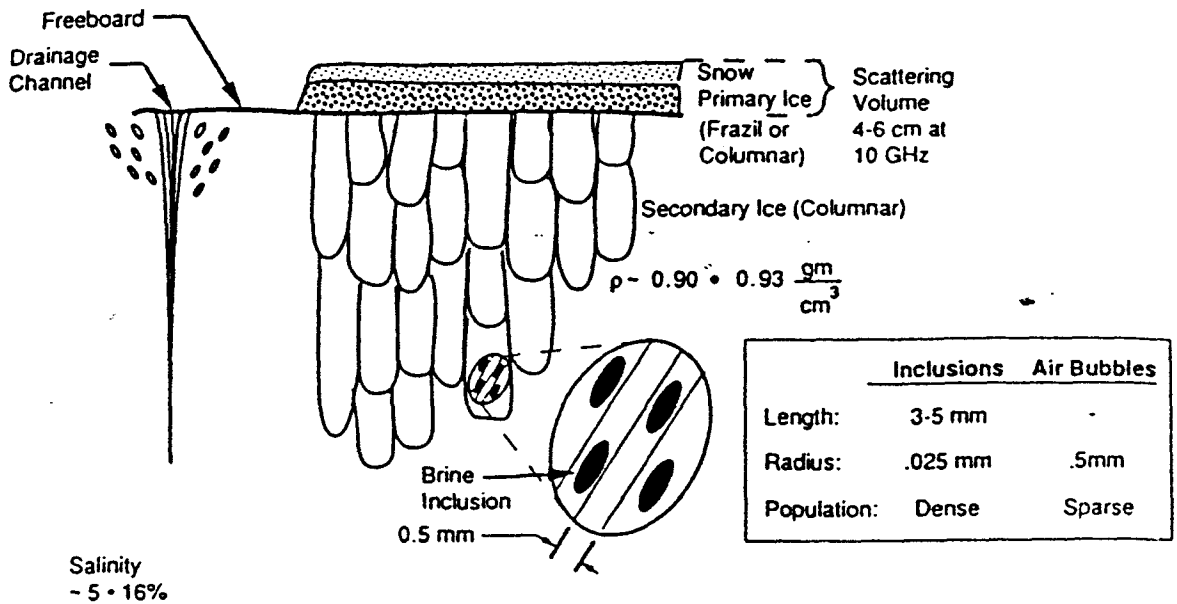
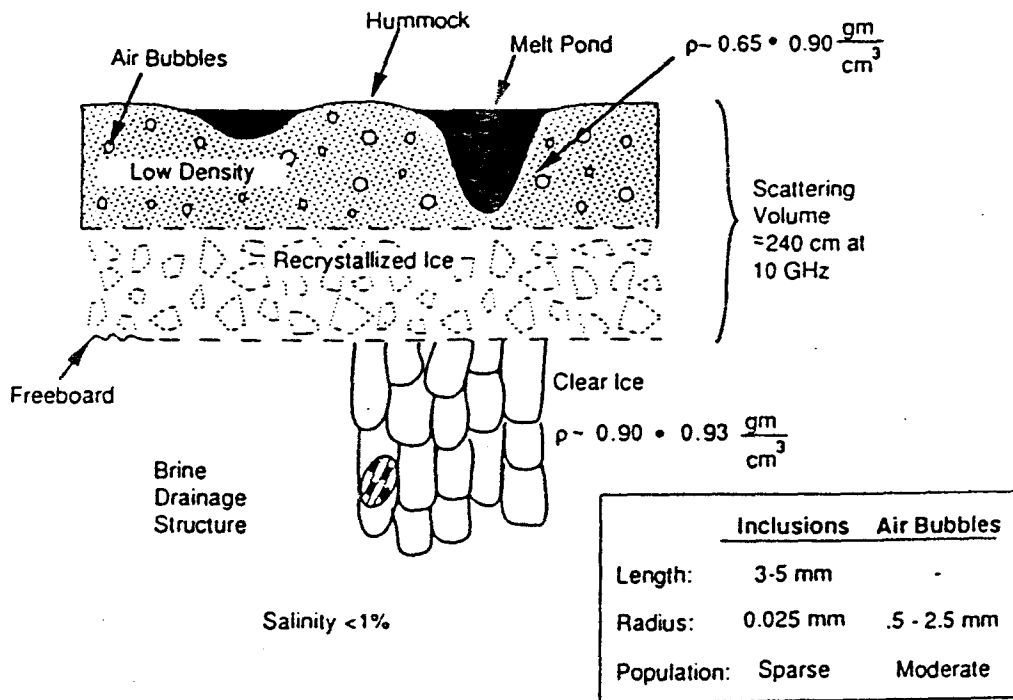


Fig. 5-3. Snow and ice conditions encountered on multiyear ice during (a) winter and early spring, (b) late spring, (c) early summer to midsummer, and (d) midsummer to late summer. Snow and ice conditions encountered on first-year ice during (e) winter and early summer, (f) late spring, (g) early summer to midsummer, and (h) midsummer to late summer [Onstott et al., 1987].



Simplified Cross Section of First-Year Sea Ice



Simplified Cross Section of Multiyear Sea Ice

Figure 3.5 Simplified cross section of first-year and multiyear sea ice.

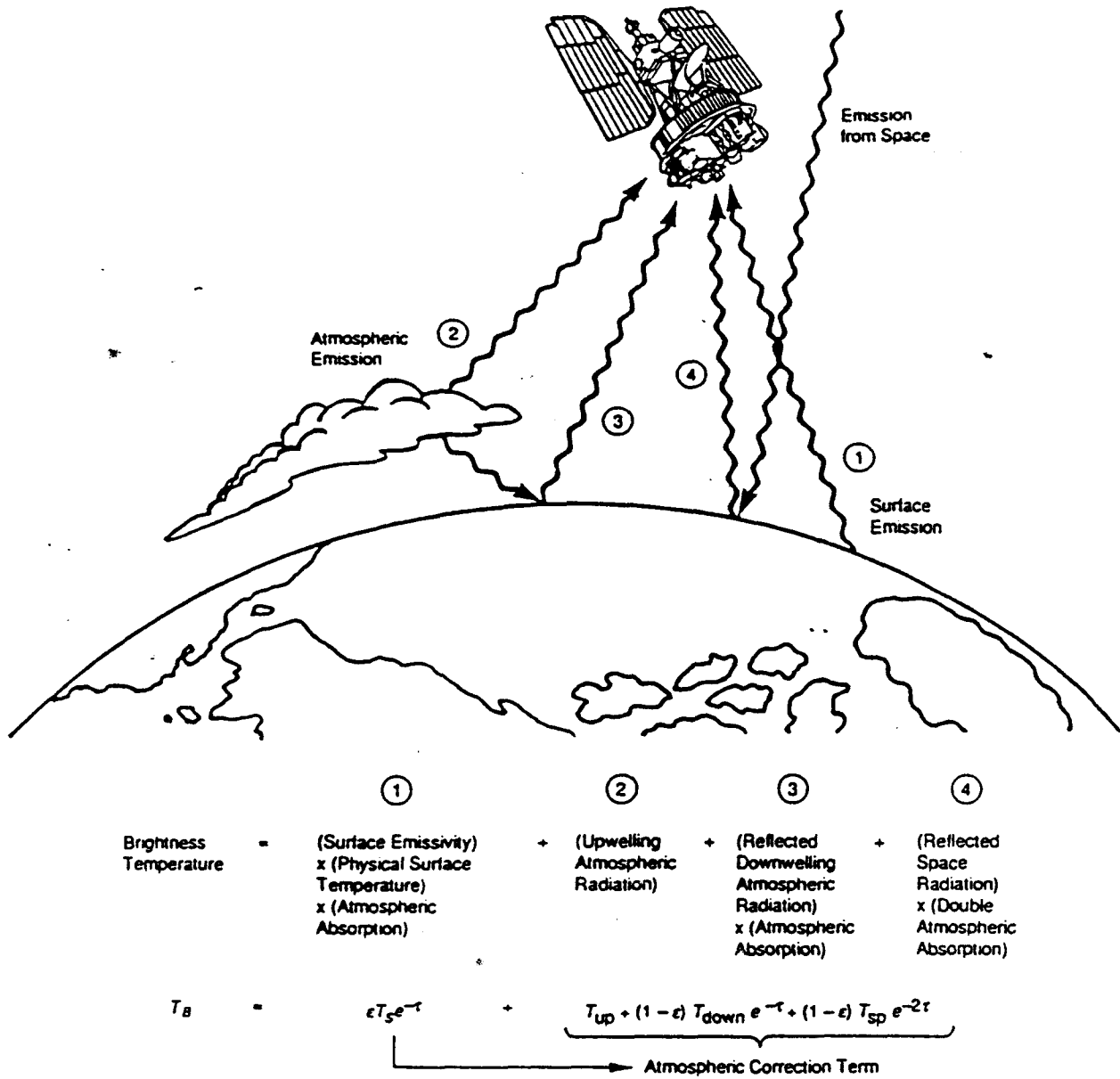


Fig. 10-1. Radiative transfer equation used to derive geophysical parameters from spacecraft microwave radiometer data [Swift and Cavaliere, 1985].

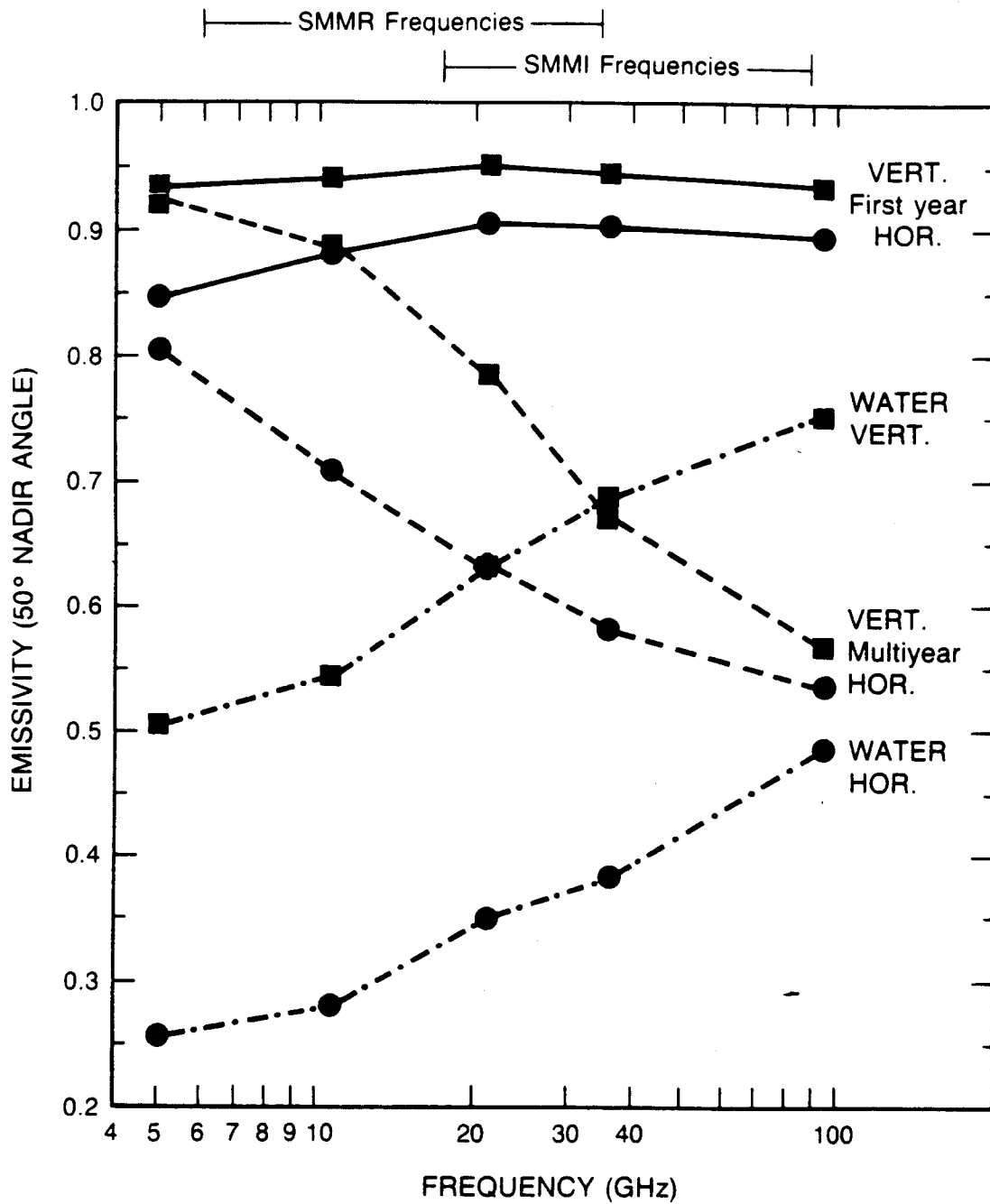


Fig. 2. Frequency dependence of electromagnetic radiation in the microwave region over sea ice (first-year and multi-year) and ocean for both horizontal and vertical polarizations (from Svendsen et al., 1983, published by the Am. Geophysical Union).

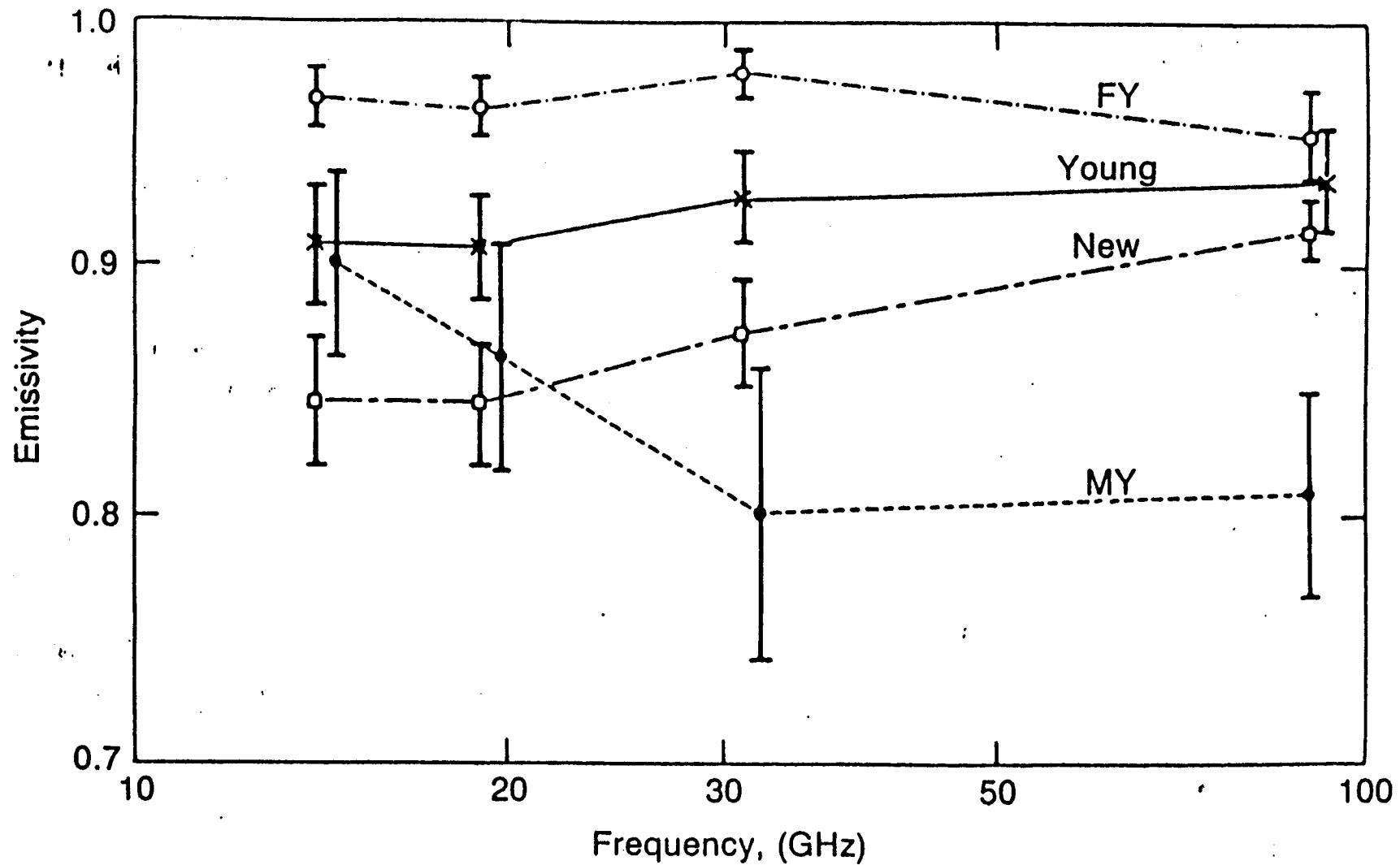
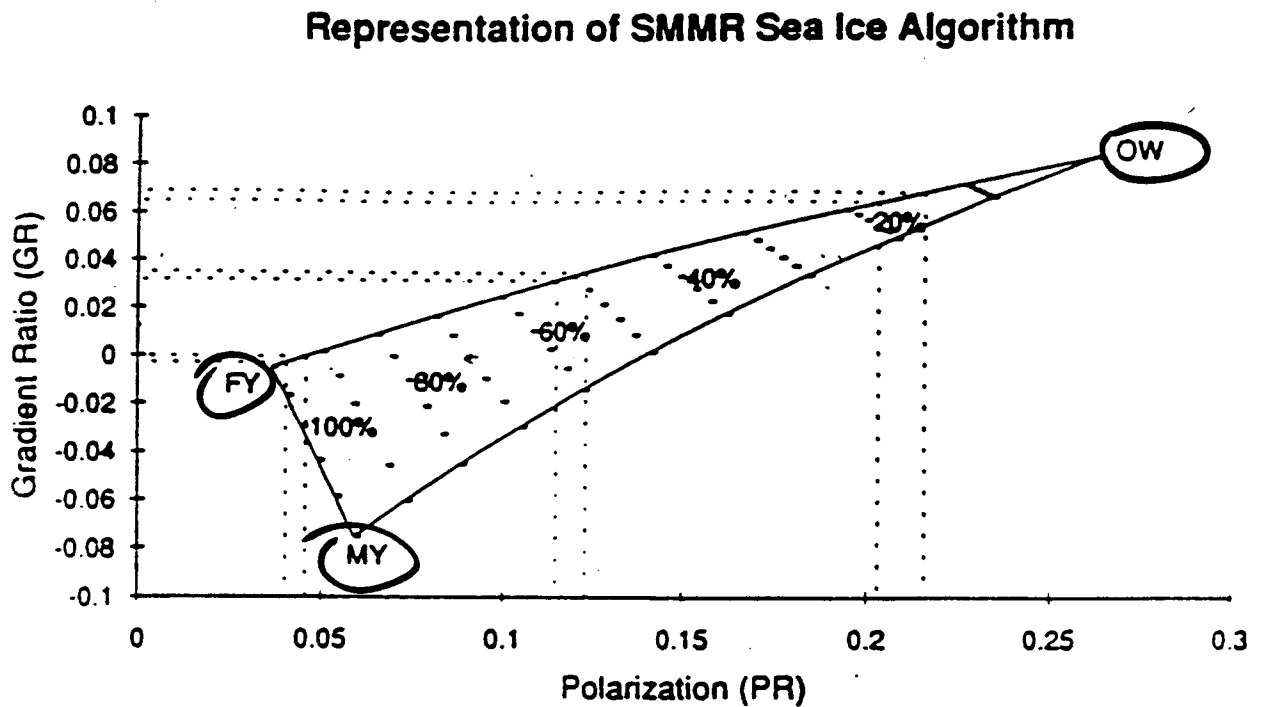


Figure 3.6 The emissivity of four Arctic sea ice types at nadir in the 14–90GHz range. Each vertical bar represents 1 standard deviation in the data, with symbols displaced to avoid overlapping. From Troy and others (1981).

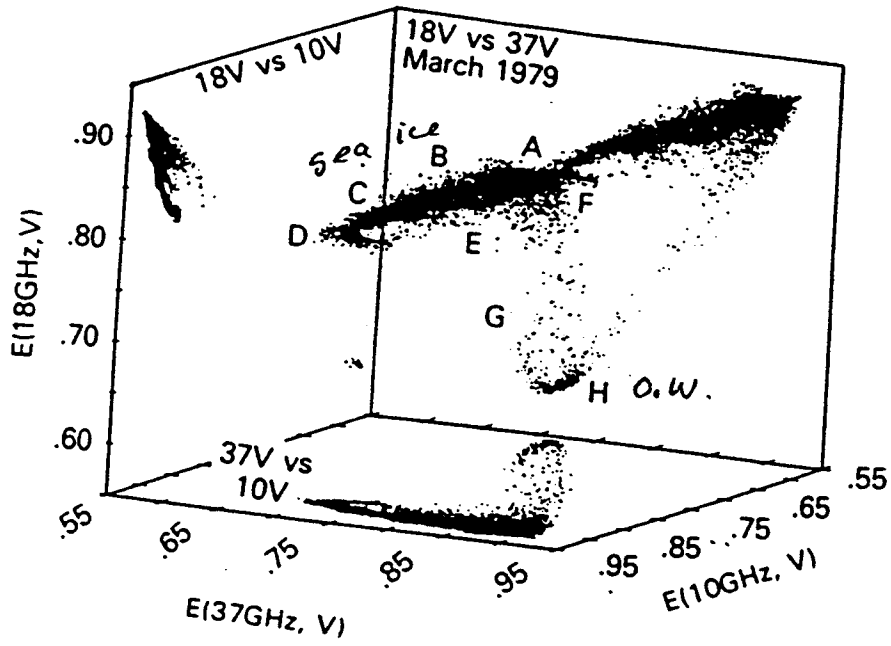
Fig. 9.6 Sensitivity of ice concentration calculations to gradient ratio and polarization variations [from Gloersen et al., 1992].



$$GR = (T_{37V} - T_{18V}) / (T_{37V} + T_{18V})$$

$$PR = (T_{18V} - T_{18H}) / (T_{18V} + T_{18H})$$

a) 10V vs 18V vs 37V



b) 18V vs 37H vs 37V

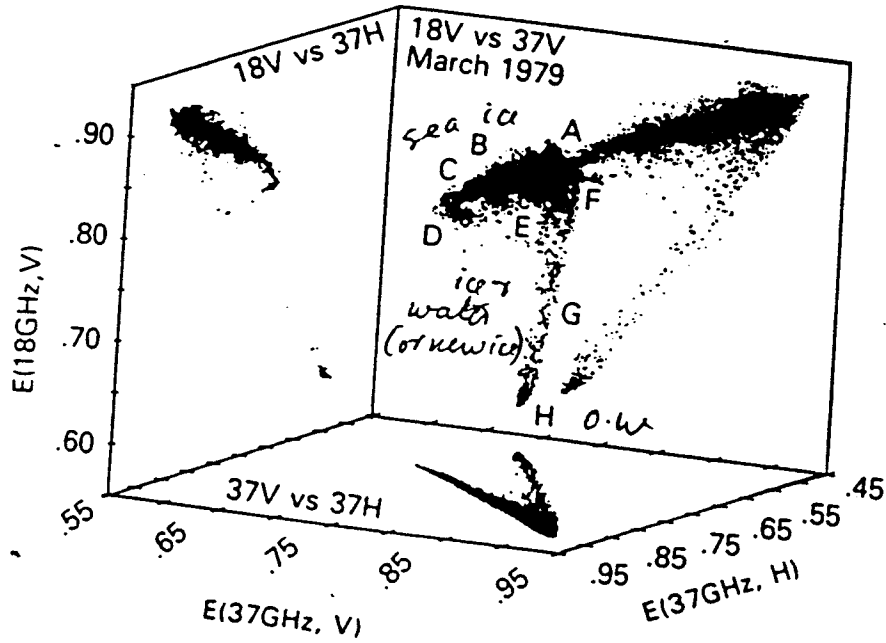


Fig. 5. 3-D Emissivity scatter plots: (a) 37V vs. 18V vs. 10V and (b) 37V vs. 37H vs. 18V (from Comiso, 1986, published by the American Geophysical Union).

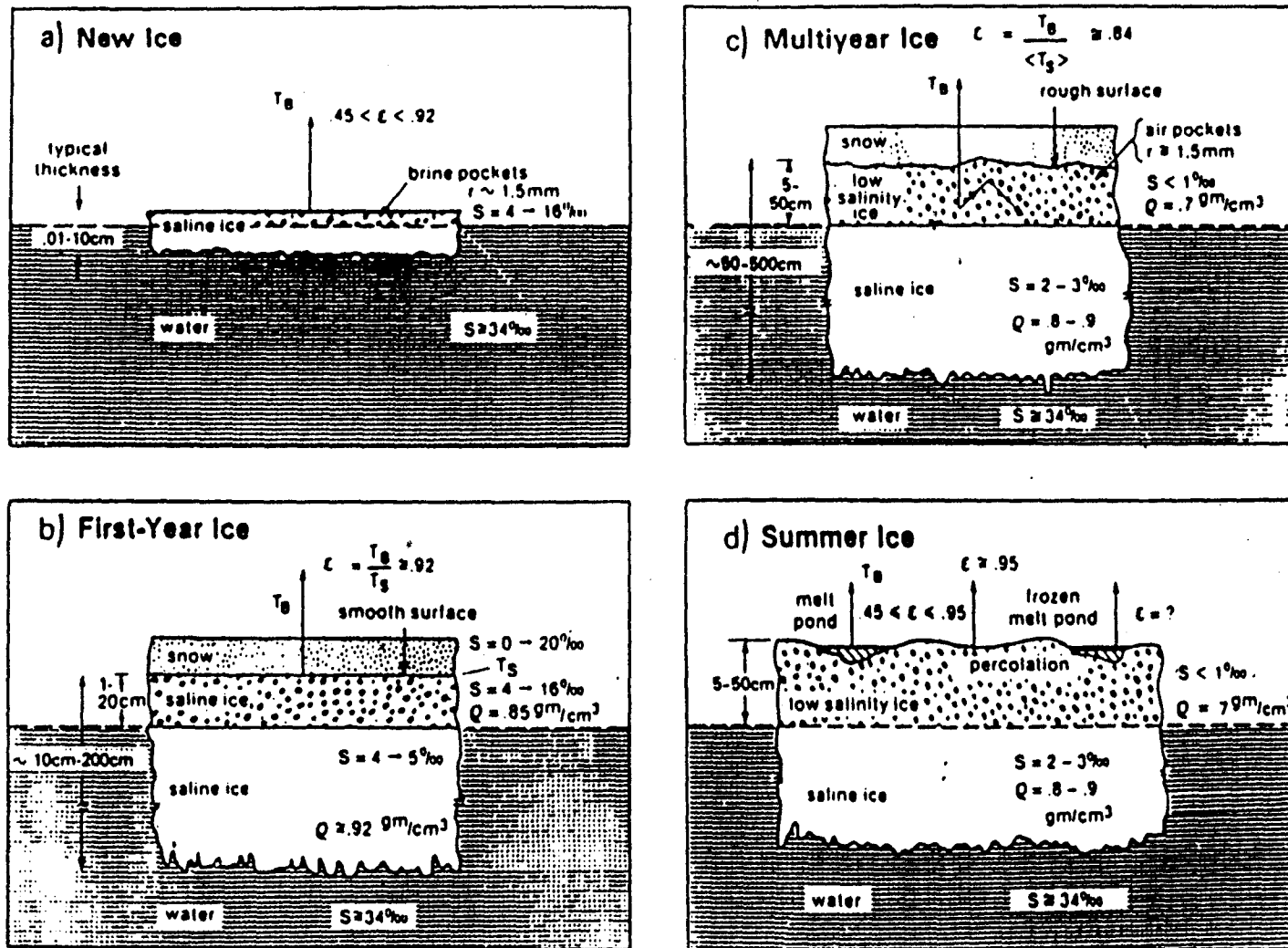


Figure 3.4 Schematic diagram of the physical properties of principal Arctic sea ice types as they affect their radiometric properties at 19.35GHz (wavelength 1.55cm). Differences in observed emissivity are caused mainly by (i) differences in ice thickness (for very thin ice); (ii) variations in dielectric properties (dependent largely on salinity, temperature and wetness); and (iii) the degree of volume scattering. From Zwally and others (1983a).

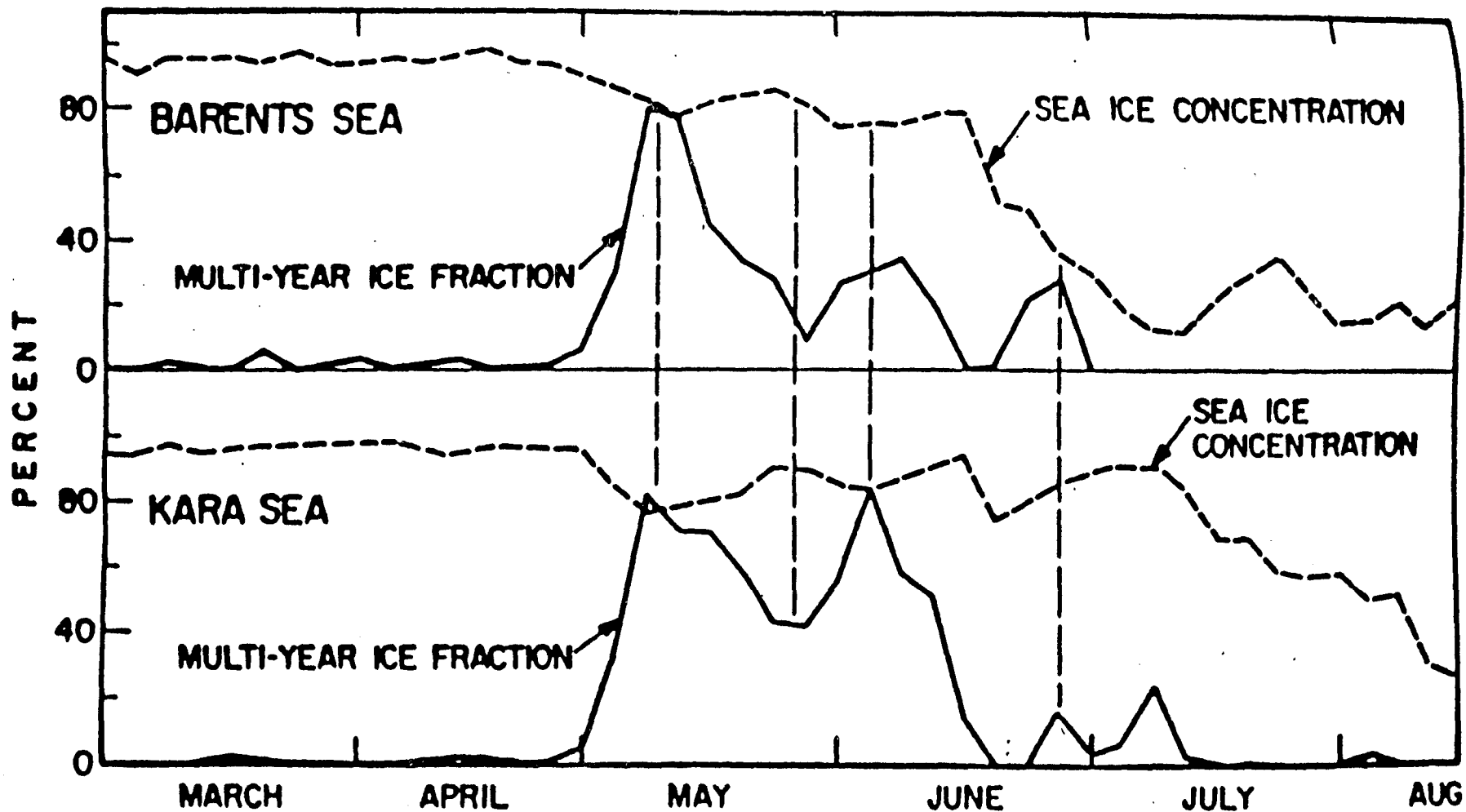


Figure 11. Time variation of sea ice concentration and multiyear ice fraction for 180 km² areas in the Barents Sea (71°N, 61°E) and Kara Sea (83°N, 45°E), March - August 1979 from SMMR data. The spurious signatures of multiyear ice are caused by melt phenomena (from Anderson *et al.*, 1985). Reprinted by permission.

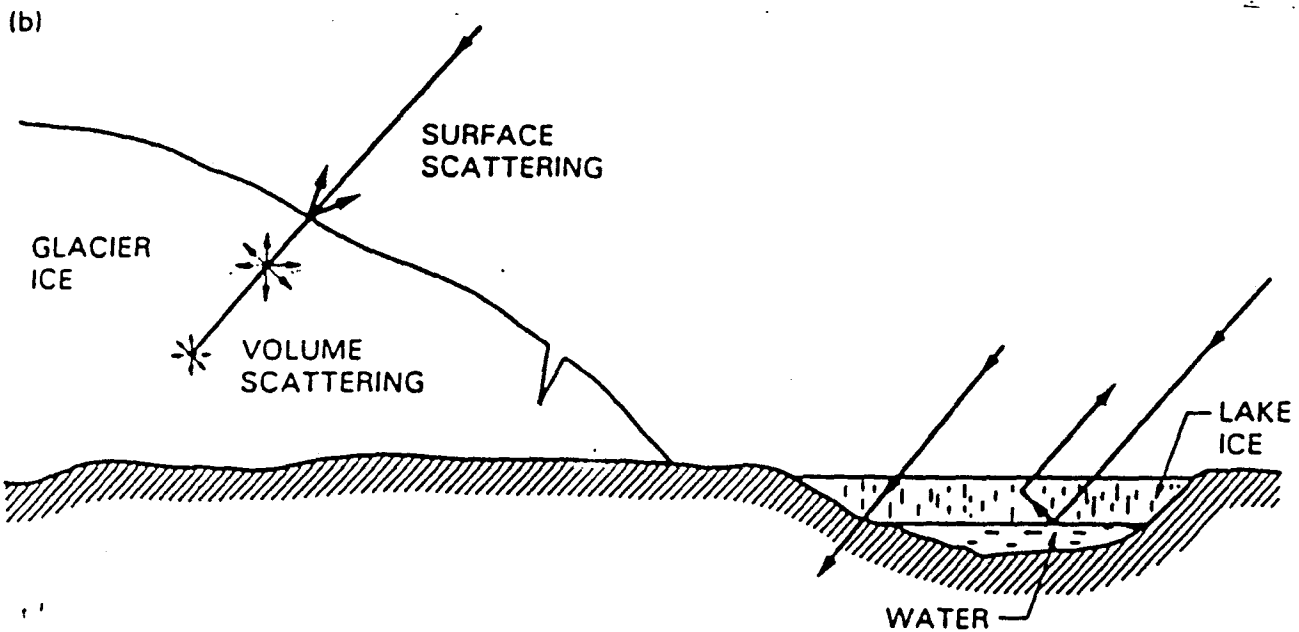
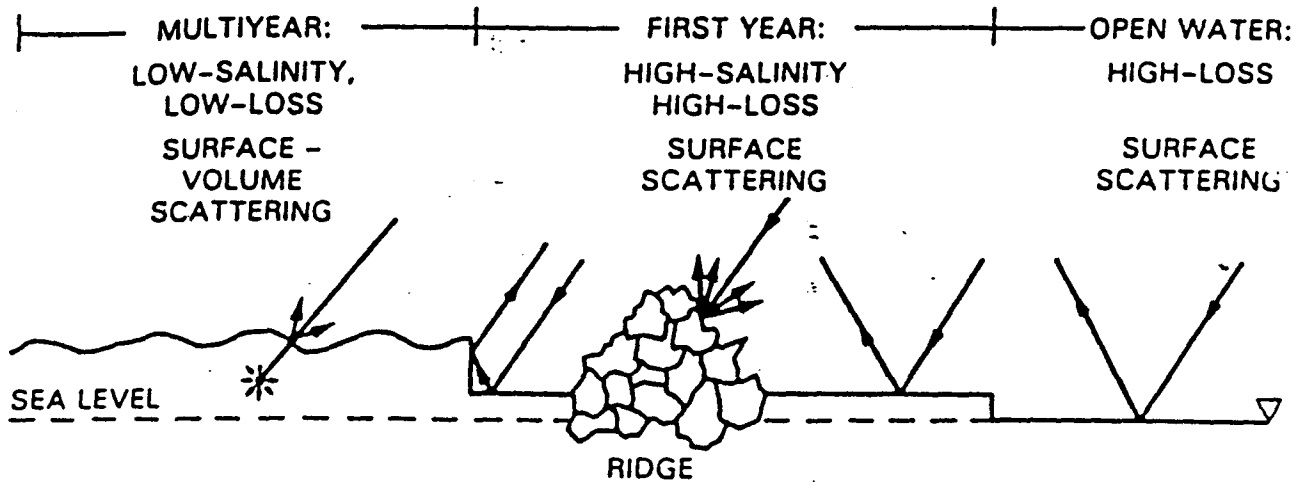


Figure 3.10 Schematic diagram of the interactions between radar and (a) sea ice, and (b) glaciers, ice sheets and lake ice. Interactions will differ at times of melt. From NASA (1987b).

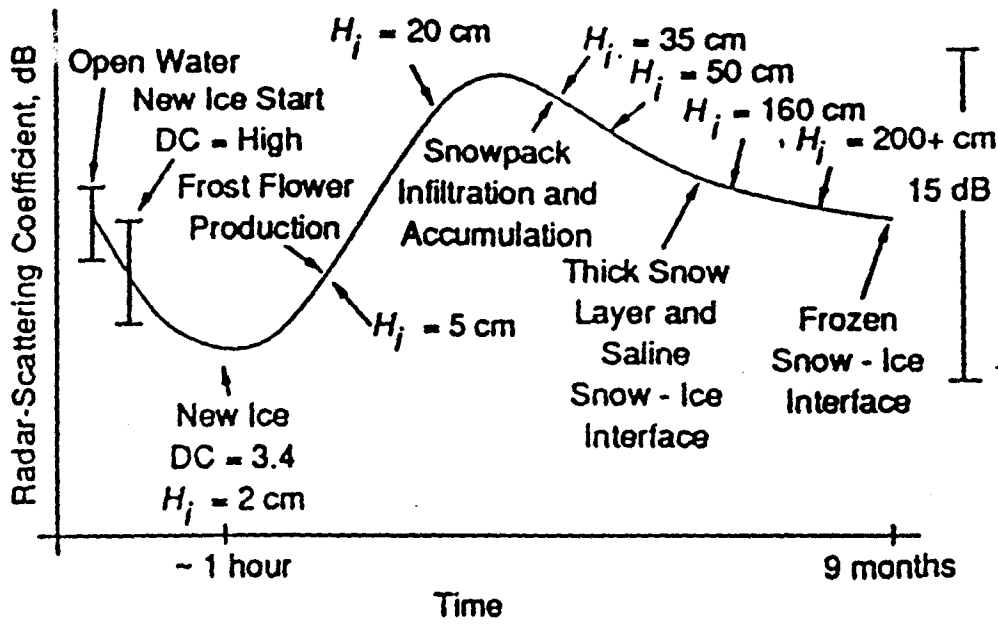


Fig. 5-21. The evolution of the microwave signature of first-year ice. (DC = dielectric constant and H_i = ice thickness.)